CHALMERS
UNIVERSITY OF TECHNOLOGY

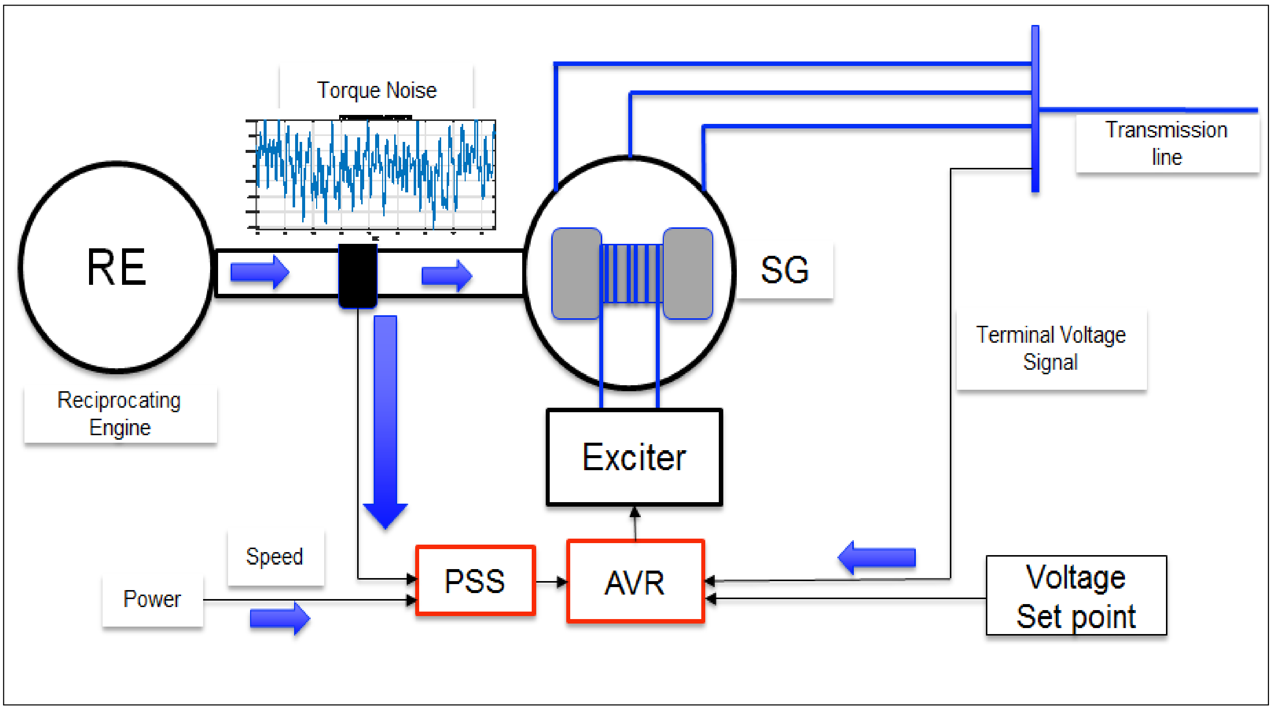

Evaluation of Methods for Improving and Testing Power System Stabilizers in Reciprocating Engines

Master of Science Thesis

ERDI HALYES & GAYATHRI RAJA

Department of Energy & Environment
CHALMERS UNIVERSITY OF TECHNOLOGY
Gothenburg, Sweden 2016

Evaluation of Methods for Improving and Testing Power System Stabilizers in Reciprocating Engines

Master of Science Thesis

ERDI HALYES & GAYATHRI RAJA

Department of Energy & Environment
Division of Electric Power Engineering
CHALMERS UNIVERSITY OF TECHNOLOGY
Gothenburg, Sweden 2016

Evaluation of Methods for Improving and Testing Power System Stabilizers in Reciprocating Engines
ERDI HALEYS & GAYATHRI RAJA

Master Thesis
Department of Energy & Environment
Division of Electric Power Engineering
Chalmers University of Technology
SE–412 96 Gothenburg
Sweden
Telephone +46 (0)31–772 1000

Evaluation of Methods for Improving and Testing Power System Stabilizers in Reciprocating Engines

ERDI HALEYS & GAYATHRI RAJA

Department of Energy & Environment
Division of Electric Power Engineering
Chalmers University of Technology

Abstract

The small-signal stability of a power system is enhanced by damping system oscillations by power system stabiliser (PSS). In synchronous generators driven by reciprocating engines there are torque variations which in turn disturb the PSS operation. This thesis investigated the current methods used to design PSS for reciprocating engines and also the use of filters to reduce the engine torque fluctuation. The use of torque change for testing PSS performance is also investigated. This is done by modelling a linearised single machine infinite bus (SMIB) along with PSS2B in Matlab as well as in Simpow software. The time and frequency domain analysis were used to evaluate the performance of the system with and without the PSS and notch filter. It is found that the proper tuning of PSS2B can improve the overall damping and stability of the system. The appropriate notch filter implementation at the frequency where the torque noise occur help to greatly attenuate the torque noise from the engine without affecting the PSS operation and overall stability. This also study shows that the deliberate torque change can be used for evaluation of PSS performance at local oscillation modes.

Keywords: SMIB, PSS/PSS2B, Torque noise, Notch filters, Stability.

Acknowledgement

Firstly, we would like to express our gratitude to our supervisor Bengt Johansson for the tireless support and guidance throughout the thesis, without whom we wouldn't be able to complete it. Then we would like to thank, Joachim Andersson for all the valuable advice and feed-backs that he gave us, which helped us complete this work. We would like to express our special thanks to Imtihaz for his help and also Erik. We would also like to thank Bengt Johansson and Sven Granfors for giving us the opportunity to do this interesting thesis work at Solvina AB.

Further, we would like to express our sincere gratitude to Tarik Abdulahovic, our supervisor and Examiner at Chalmers, for his thoughtful suggestion and support throughout the thesis. Thank you so much.

Last but not least we would like to thank all Colleagues at Solvina AB and all the faculty and staff at Chalmers University.

Erdi & Gayathri

Gayathri: I would like to thank my husband for the constant encouragement and moral support given during my master's studies and also my parents and friends.

Erdi: I would like to thank my family and friends, for their non-stop support to make me the person I am now. Thank you very much.

Gothenburg, 2016

Contents

List of Figures

List of Tables

Abbreviations

AVR	Automatic Voltage Regulators
DSL	Dynamic Simulation Language
DYNPOW	Dynamic Power Flow
GM	Gain Margin
IEEE	Institute of Electrical and Electronics Engineers
OPTPOW	Optimal Power Flow
PM	Phase Margin
PSS	Power System Stabilizers
RTF	Ramp Tracking Filter
SMIB	Synchronous Machines Infinite Bus
STAPOW	Static Power Flow

1

Introduction

Stable operation of power systems is very important for optimal transfer of power from generation to load. With the increasing size of power system networks, synchronous machines often experience stability problems created because of different reasons. For example; line faults, short circuit conditions, over/under-loading conditions, synchronizations problems [1], addition of renewable energy sources [2] and so on. For a small disturbance, the ability of power system to remain synchronised is defined as small signal stability [1].

Normally, in excitation systems the Automatic Voltage Regulators (AVR) controls the air gap flux produced by the field generator which in turn controls the terminal voltage. In many power systems Power System Stabilizers (PSS) are used together with AVR of the synchronous generators to improve its performance. A PSS is a feedback control systems whose main function is to provide additional damping for small disturbances. PSS often sense either electrical power produced, terminal frequency or shaft speed in order to measure the rotor disturbances and hence produce an additional signal to the AVR, thereby improving the synchronous machines dynamic performance [1]. In traditional PSS, these input signals are often passed through a series of lead/lag filters. This is done in order to provide phase compensation.

It is required in many countries that all power plants shall be equipped with PSS in order to reduce oscillations. This is because PSS can improve a power system in many different ways, for example, stabilize the system, ensure a margin of stability over a wide range of operation and increase the power transfer capability[3]. The PSS must be able to compensate for the phase introduced by the AVR, exciter and the field generator in order to improve the amount of damping present in the system [4].

Reciprocating engines (piston engines, gas or diesel) are used in many power plants globally, often in combination with renewable power such as wind or solar power. In generators driven by reciprocating engines, there are often engine torque fluctuations which disturb the operation of PSS. These oscillations are mainly in the range of 1 to 10 Hz, hence can be normally categorized under small signal stability analysis[3].

1.1 Problem Description

When designing a PSS it is desirable to have as high gain as possible in order to have high damping[1]. In reality torque noise created from the reciprocating engine creates problems in PSS thus disturbing its proper operation. Hence, this disturbance has to be filtered without affecting the system stability. Several investigations were conducted in order to study the use of filters of mitigation of the disturbances. However, many of the papers deal with torsional oscillations, where noises originate from interactions between parts of the turbine. Whereas in this case, the source of the noise is the engine torque itself.

Even though filters can be used to remove these noises, addition of filter components introduces further phase distortion in the PSS control loop. It is common to use low pass, band pass or band reject filters to suppress noise. If the filters are not properly designed and investigated they could create further problems. Generally, the higher the noise the higher the attenuation should be. At the same time, this introduces a higher phase lag or lead in the system, which is not desirable. This implies that the amount of phase compensation provided by the PSS lead-lag filters will be limited due to their phase-magnitude characteristics. It is also crucial to study the effect of these filter on the phase and gain characteristics as well as the stability of the system as a whole.

1.2 Aim

The aim of the thesis is to investigate the current methods used in PSS design for reciprocating engines and to make possible improvements that can be done to overcome torque noise problems. This includes the use of filters for reducing disturbances from engine torque variations as well as the use of these torque variations for testing PSS performance.

1.3 Method and Scope

The primary work involves modelling of the classical and most commonly used model for small signal stability studies which is synchronous machines infinite bus model (SMIB) [3]. A PID type AVR with brushless rotating exciter and PSS2B is modelled and implemented using standard IEEE models.

The modelling includes the parameter tuning of the AVR and PSS. The problem with design of PSS in reciprocating engines is their susceptibility to torque noise. For this, a case study is conducted with real time data provided by Solvina AB. The

PSS parameters are tuned accordingly, so that the overall system remains stable. Filter design is investigated and suitable filter is implemented to mitigate the torque noise. Most of the frequency domain analysis is conducted in Matlab using Simulink control system toolbox. The effect of deliberate torque changes to the performance of PSS is investigated as well. Simpow is used to verify the model in frequency domain as well as time domain analysis.
The main limitations of this thesis are:

- Only the IEEE model of PSS2B PSS is studied. This is because of its basic and simple design as well as its ability to replace the dificult mechanical power measurement by speed (or frequency) and electrical power.
- Mainly notch filters are investigated as it is found to be the best option to filter noise at a particular frequency as well as their easy implementation and comparatively lower phase addition compared to band reject filters. This is done by comparing filters of different depth and bandwidth.
- The simplified model of turbine and governor models are used in Simpow, but not in Matlab. This is because the response of the governors is slow comparing to the range of oscillation frequencies where the PSS operates [5] in a linearized system. Since a linearised model is used in Matlab the limiters can be neglected and used in Simpow only.

2

SMIB system modeling

2.1 Introduction: small signal stability

Small signal stability concerns whether a system stabilises after a disturbance. The small-signal stability or disturbance is due to the switching on or off small loads which in-turn varies the generation by a small amount. This is a common and continuously process in a system. Due to the small-signal disturbance there are oscillations having different characteristic response and frequency often referred as modes of oscillations. Some of the modes of oscillation are [1], [3] :

- Local modes - where a generator swing against the rest of power system and the frequency lies in the range of 1-3Hz.
- Inter area mode - where group of generator swing against another group of generator and frequency lies in the range 0.25-1 Hz
- Torsional modes - these are associated with turbine prime mover and the generator shaft and frequency is generally greater than 8Hz.

2.2 Power system representation

The single line diagram shown in Figure 2.1 represents a SMIB system model developed by Heffron and Phillips. Representing the network with a Thevenin's equivalent circuit at the connection point will reduce the system presented in Figure 2.2, where E_t is the generator bus voltage and Thevenin's voltage E_B represents the infinite bus voltage. In this model, the infinite bus voltage is assumed to be constant even at the occurrence of changes in generator G_1. This is true unless some parameter changes occur in the infinite bus itself [1]. After introduction of the primary synchronous machine model, each component of the system including the control system is modelled. Their effect on the whole system performance is then studied.
The SMIB system represented in Figure 2.2 is the standard model used in power systems stabilizer tuning studies.

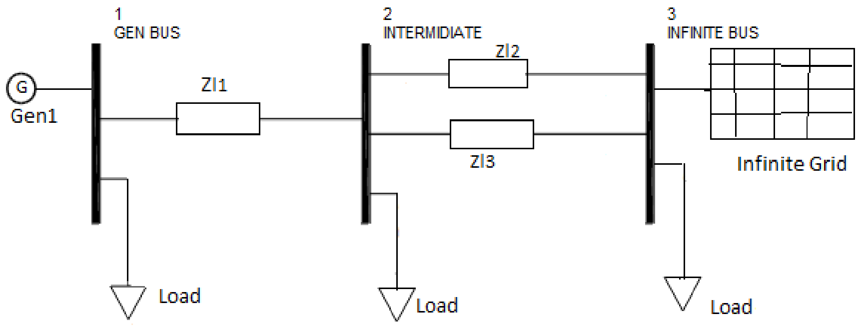

Figure 2.1: Single line diagram of a SMIB system

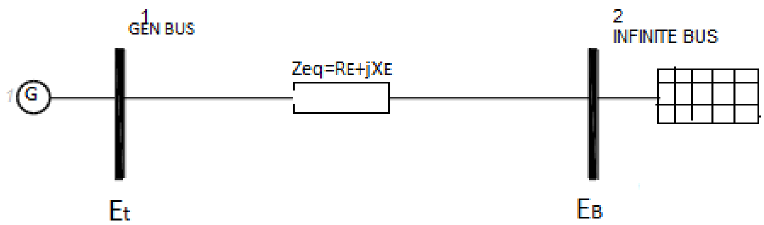

Figure 2.2: Reduced single line diagram of a SMIB system

The mechanical and electrical dynamics of this system is modelled in the coming sections. Since the main focus of this thesis is small signal stability performance of the system with regard to PSS tuning and filtering of torque noise, a model linearized around the steady-state operating point is sufficient for small-signal analysis purposes [3]

2.3 SMIB Modelling

The generator is represented by the transient reactance X'_d for performing dynamic simulations [6], and terminal voltage E_t, where δ is the angle between the generated voltage $E'$and the infinite bus voltage E_B at the steady-state operation. Current I_T is flowing from generator into the network.

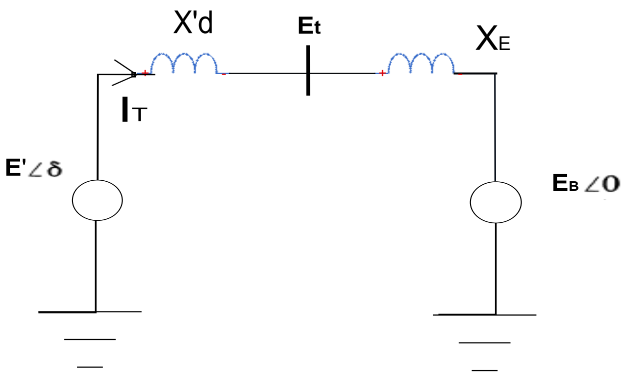

Figure 2.3: Classic generator infinite bus single line diagram

Observing Figure 2.3 the electrical parameters of the system can be calculated as:

$$I_T = \frac{E' \angle \delta - E_B \angle 0}{X_T} \tag{2.1}$$

and

$$P_e = \frac{E' E_B}{X_T} sin(\delta_0) \tag{2.2}$$

,where $X_T = X_d{}' + X_E$ is the total reactance from the generator to the infinite bus and δ_o the initial rotor angle.

For small perturbations expressed in per-unit the electrical power is equal to the air gap torque. One new term can be defined, which is the synchronizing torque coefficient that is in phase with the rotor angle deviation [1].

$$K_s = \frac{E' E_B}{X_T} cos(\delta_o) \tag{2.3}$$

Hence, the linearized mechanical dynamics of the synchronous machine can be represented by the equation of motion

$$p\Delta\omega_r = \frac{1}{2M}(\Delta T_m - \Delta T_e - \Delta T_D) \tag{2.4}$$

and

$$\Delta\omega_r = (\frac{1}{\omega_o})p\Delta\delta. \tag{2.5}$$

The notation p is a differential operator, ΔT_m represents mechanical input torque perturbations. Similarly, ΔT_e is the air gap torque perturbation while ΔT_D is the damping torque. M is Moment of inertia of the machine and it is twice as large as the inertia constant H. $\Delta\omega_r$ is rotor speed deviations in radian per unit and $\Delta\omega_o$ is steady state synchronous speed of the machine. Finally rotor angle perturbations in electrical radians is represented as $\Delta\delta$.

Equations (2.4) and (2.5) are used to develop the basic relationship of the SMIB model. The state-space matrix of the model in Figure 2.3 is given below where the the states of the system are perturbations in speed $\Delta\omega_r$ and change in initial rotor angle $\Delta\delta$. The states of the machine dynamics depend on parameters such as H, which is constant and does not change with system operating conditions. However parameters K_D and X_T varies with change in the system operating conditions[1]. The block diagram given in Figure 2.4 represent a simple synchronous generator without the effect of field as well as damper winding dynamics in frequency domain.

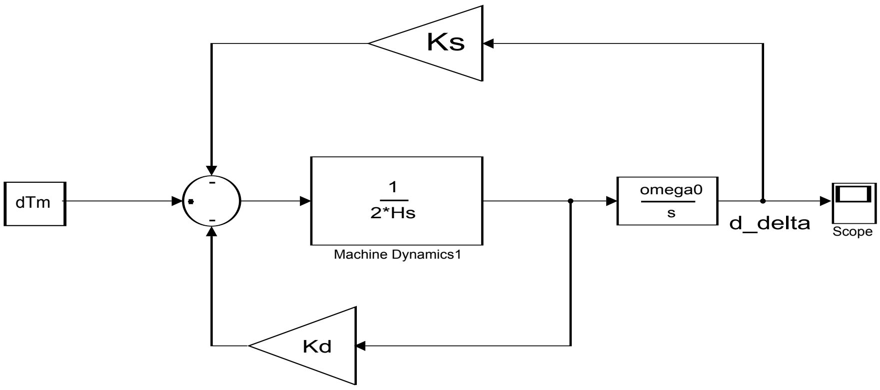

Figure 2.4: Second order model of synchronous machine

$$\begin{bmatrix} \dot{\Delta\omega} \\ \dot{\Delta\delta} \end{bmatrix} = \begin{bmatrix} \frac{-K_D}{2H} & \frac{-K_s}{2H} \\ \omega_o & 0 \end{bmatrix} \begin{bmatrix} \Delta\omega \\ \Delta\delta \end{bmatrix} + \begin{bmatrix} \frac{1}{2H} \\ 0 \end{bmatrix} \Delta T_m \tag{2.6}$$

In the state-space equation given in (2.6) ΔT_m represents the change in the input mechanical torque or power to the system. Inherent system characteristics can be found from the second order characteristic equation of the state space. The undamped natural frequency ω_n and the damping ratio ξ of the undamped oscillation can be calculated :

$$\omega_n = \sqrt[2]{(K_s \frac{\omega_o}{2H})} in rad/sec \tag{2.7}$$

$$\xi = \frac{0.5 K_D}{\sqrt[2]{2HK_S\omega_o}}, \tag{2.8}$$

where $\omega_o = 2\pi f_0$ in rad/sec and f_o is initial synchronous machine (grid) frequency. In addition, the damped frequency of oscillation can be found from the damping ratio using the relationship:

$$\omega_d = \omega_n \sqrt[2]{1 - \xi^2} \tag{2.9}$$

Hence it can seen from (2.7) and (2.8) the synchronizing torque coefficient is directly proportional to the square of the undamped natural frequency. The damping torque coefficient K_d is directly proportional to the damping ratio.

2.4 Excitation System and AVR modelling

Different books define excitation system in different ways. As per [3] it refers to components consisting of field generator that generates field voltage, field regulation control system for regulation of reactive power, terminal voltage and a set of protective elements encompassed along with it. Similarly [7] refers the excitation system to the AVR that produces a control signal for the field generator. This is done through the feedback system which compares the reference voltage and the feedback signal derived from the measurement of the terminal voltage. The error signal is fed to the control system of the exciter in order to set the proper field.

The excitation system has several important function which among them is providing a compensation signal for overcoming different modes of oscillations within the system [1],[3]. In a typical power system oscillating at any frequency, the excitation system controls the torque component which can be in phase with the synchronous machine's rotor angle perturbations or the machines rotational speed [8].
A simple and linearized field winding model is developed which is lumped to the previous explained model 2.4, followed by the AVR general model. The typical IEEE standard PID type AVR with rotating brush-less exciter is employed in the later stages for simulations.

2.4.1 Modelling of Field winding

A simplified field winding is considered for the system stability studies. Accordingly, the effect of damper winding are neglected. It is also assumed that the AVR is set to manual control (where reference voltage remains constant).

Primarily the infinite bus voltage and the field circuit equation is transformed into the dq reference frame (appendix A). The state space model of the exciter and the generator and mathematical derivation of the constants of model is given in appendix (A.8) and represented by the block diagram in 2.5 .

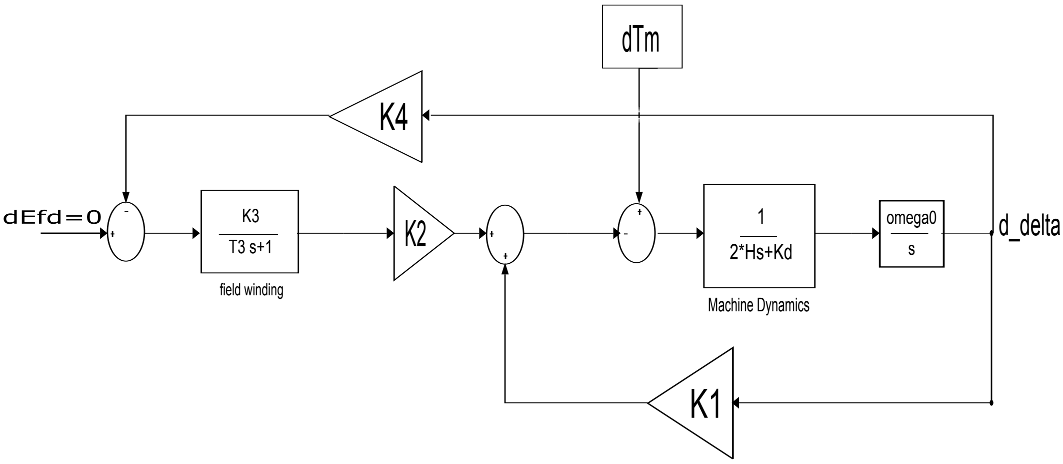

Figure 2.5: Synchronous machine with field dynamics

As can be seen from the block diagram presented in 2.5, four constants $K1, K2, K3$ and $K4$ know as Heffron Phillips constants are introduced. The effect of field variations in the machines dynamics and torque components is better viewed from the block diagram shown in Figure 2.5. Assuming the excitation system (AVR) is on manual control mode, where ΔE_{fd} in Figure 2.5 is zero, the variations in generator flux linkages are created only due to the change in rotor angle feedback through the constant K_4. The closed loop transfer function between the input torque of electromagnetic origin and the rotor angle is calculated as (2.10).

$$\frac{\Delta T_e}{\Delta \delta} = K_1 - \frac{K_2 K_3 K4}{1 + sK_3 T'_{d0}} \tag{2.10}$$

,where $T'_{d0} = K_3 T_3$. According to [8], for a stable operation of the synchronous machine, the excitation system should be able to provide a positive synchronizing and damping torque to interact the oscillation arising due to change in the rotor angle and speed. The observation from (2.10), is that at certain rotor oscillation frequencies, the system will be stable when the field generator completely compensates for the demagnetizing effect of the armature reaction at the input of the synchronous machine [9]. That means the field winding contributes positive damping at higher rotor oscillation frequencies and zero damping at steady state [1]. Even though the constant K_4 is mostly positive, under special conditions of high loading at remote distances [10] or high resistance to reactance ratio [11], the constant K_4 can be negative which could contribute to system instability.

2.4.2 AVR Modelling

The AVR maintains the terminal voltage by proving control signals to the exciter, which in-turn provides a current to synchronous machine's rotor field winding,

thereby improving the system stability [12]. In a real system the AVRs are accompanied with limiters to protect the generator, excitation system and grid from reaching saturation and the terminal voltage from going infinitely high.
The terminal voltage of the generator, E_t, can be expressed using the state variables (with small perturbations).

$$\Delta E_t = K_5 \Delta\delta + K_6 \Delta\psi_{fd} \tag{2.11}$$

The constants K_5 and K_6 formulas are given in appendix in detail. Equation 2.11 expresses the terminal voltage error, which is forwarded to voltage transducer. The output of voltage transducer, with small perturbation is $\Delta v_1 = dV_t$, which is compared to the voltage reference signal V_{ref} and is used as an input to the AVR. This signal is used to change the exciter output and accordingly the generator field current. The first order state-space model is given in appendix (A). In order to add the effect of excitation system, the new state variable Δv_1 is introduced. With the effect of excitation system included the field circuit equation developed in the section 2.4.1 is equal to:

$$p\Delta\psi_{fd} = b_{31}\Delta\omega_r + b_{32}\Delta\delta + b_{33}\Delta\psi_{fd} + b_{34}\Delta v_1 \tag{2.12}$$

,where the constants
$b_{34} = -c_{32}K_A = -\frac{\omega_r R_{fd}}{L_{adu}}K_A$; $G_{ex}(s) = K_A$ is the exciter gain.
With mechanical torque input, $\Delta T_m = 0$ and the new state variable is given by

$$p\Delta v_1 = b_{41}\Delta\omega_r + b_{42}\Delta\delta + b_{43}\Delta\psi_{fd} + b_{44}\Delta v_1 \tag{2.13}$$

and the new states of the system can be expressed in terms of constants as: $b_{41} = 0$, $b_{42} = \frac{K_5}{T_R}$, $b_{43} = \frac{K_6}{T_R}$, $b_{44} = -\frac{1}{T_R}$ and T_R is terminal voltage transducer time constant.

The final state space representation of the system is given in the appendix (A) and the block diagram is represented in Figure 2.6.

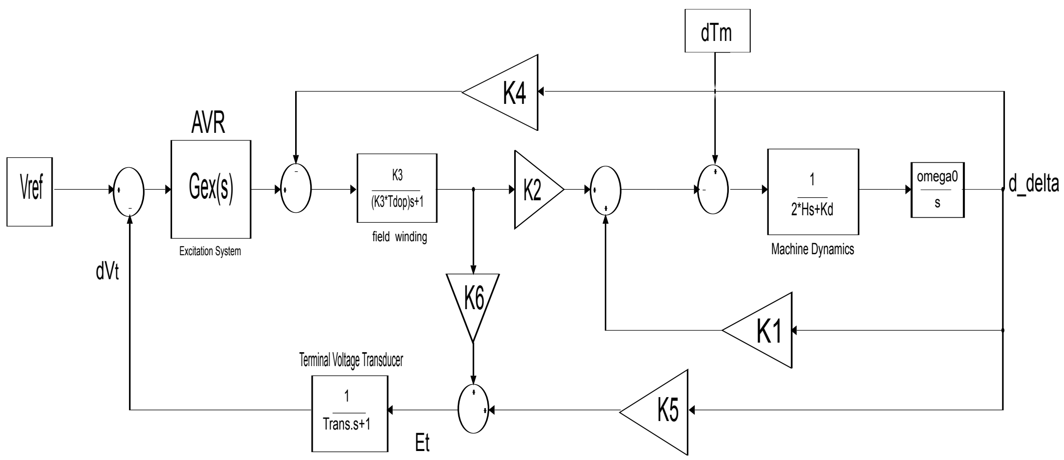

Figure 2.6: Block diagram of system with AVR

From the block diagram representation shown in Figure 2.6, the field flux is given as,

$$\Delta\psi_{fd} = -\frac{(K_3K_4 + sT_RK_3K_4) + K_3K_5G_{ex}(s)]}{s^2T_3T_trans + s(T_3 + T_{trans}) + 1 + K_3K_6G_{ex}(s)}\Delta\delta \tag{2.14}$$

In general, the coefficients K_2,K_3 and K_6 are positive. K_4 is already discussed in the previous section, while K_5 can have either positive or negative value depending on the exciter response and generator output.

It can be observed from the block diagram representation in Figure 2.6 that the constant K_1 provides a pure damping torque component which is in phase with the rotor angle deviation to the inherent damping of the machine. Hence the total damping and synchronizing torque components provided by the AVR during different rotor angle modes of oscillation can be calculated.

$$\frac{\Delta T_e}{\Delta\delta} = K_1 - \frac{(K_2K_3K_4 + sT_RK_2K_3K_4) + K_5G_{ex}(s)]}{s^2T_3T_{trans} + s(T_3 + T_{trans}) + 1 + K_3K_6G_{ex}(s)} \tag{2.15}$$

Hence, the inherent effect of the AVR on damping torque and synchronizing torque depends on K_5 and $G_{ex}(s)$ [1],where G_{ex} is the gain of the static thyristor exciter type ST1A taken into consideration as an example for illustration purpose. This notion implies that whenever the exciter response is increased in order to enhance the synchronizing torque and hence the transient stability in situation where K_5 is negative, it may introduce an unnecessary negative damping [1] or the opposite is true as well. Hence, a feedback loop containing the PSS is introduced between the generator speed and the AVR input to meet the requirement of high synchronizing torque without affecting or even enhancing the damping torque component.

The AVR frequency response performance is very important in tuning the PSS that is going to be explained in later stages. This is because if the PSS is to provide damping in addition to that of the AVR, it has to be able to compensate the phase lag that is introduced between the AVR input and the electromagnetic torque[3].

A PID type AVR with a brushless rotating exciter is used in this Matlab simulation which is given in Figure 2.7. A typical bode plot for this system is shown in Figure 2.8. The simulation result is done from the reference voltage to the terminal voltage.

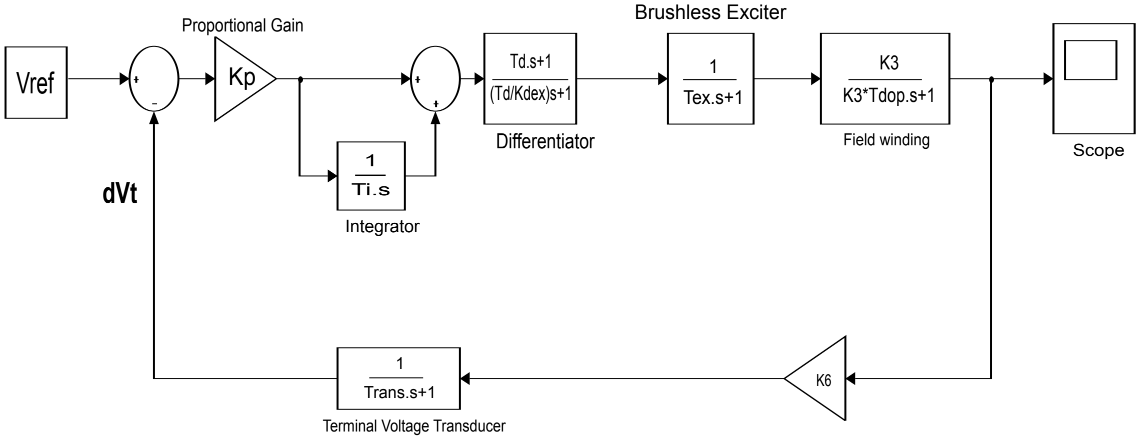

Figure 2.7: PID type AVR simulink block diagram

The term G_{ex}(s) in 2.15 is substituted by the transfer function of the AVR given as a block diagram in Figure 2.7. The generator is assumed to be offline, that is disconnected from the grid but running at rated speed. The frequency response of the excitation system taken from reference voltage to terminal voltage, assuming no change in terminal voltage, is shown in Figure 2.8.

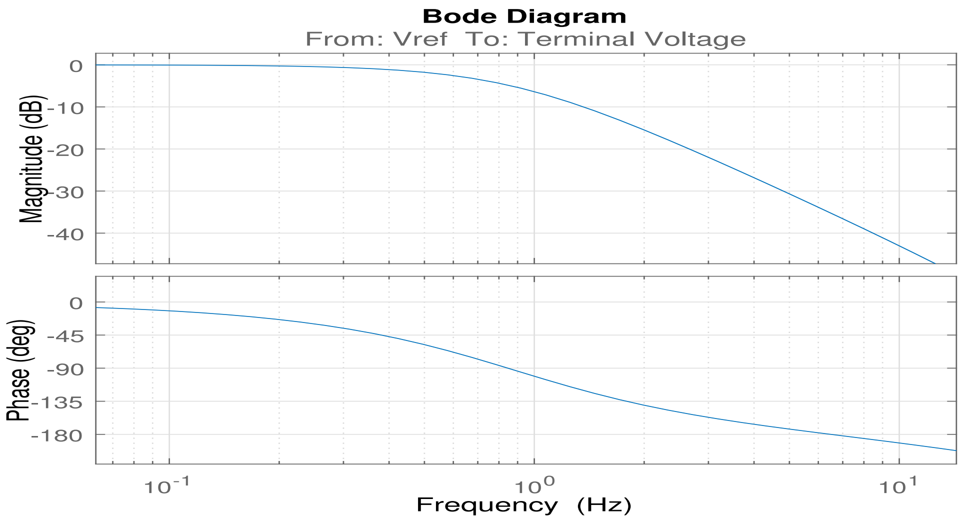

Figure 2.8: Bode plot of PID type AVR for signal taken from reference voltage to generator terminal voltage when generator is offline

It is evident from Figure 2.8, that the phase is -90 degree at local modes around 1 Hz and keep on increasing to negative with increase of frequency. Similarly, the gain decreases with increase in frequency.

2.4.3 Power System Stabilizer

Major need for power system stabilizers appeared in the United States west coast due to the need of transmitting maximum power through transmission lines. This became difficult due to inter-area mode of oscillations between groups of units oscillating against other groups [13]. Hence the PSS came in action as a feedback control loop to that aid the AVR help damp out these oscillations and improving the stable operation of a synchronous machine, thus improving power transmission capability.

Even though the main function of the Power System Stabilizer is to improve or add a damping torque component, it may with proper tuning also add a small amount of synchronizing torque. In order to be able to add damping, the torque component provided by the PSS must be in phase with the speed deviations[1] at the modes of oscillations of interest. The whole block diagram representation of the system including the PSS which is represented with the block diagram notation $Gpss(s)$ is given in Figure 2.9. The output of the PSS is added to the input of the AVR along with the reference signal and the measured voltage from the transducer.

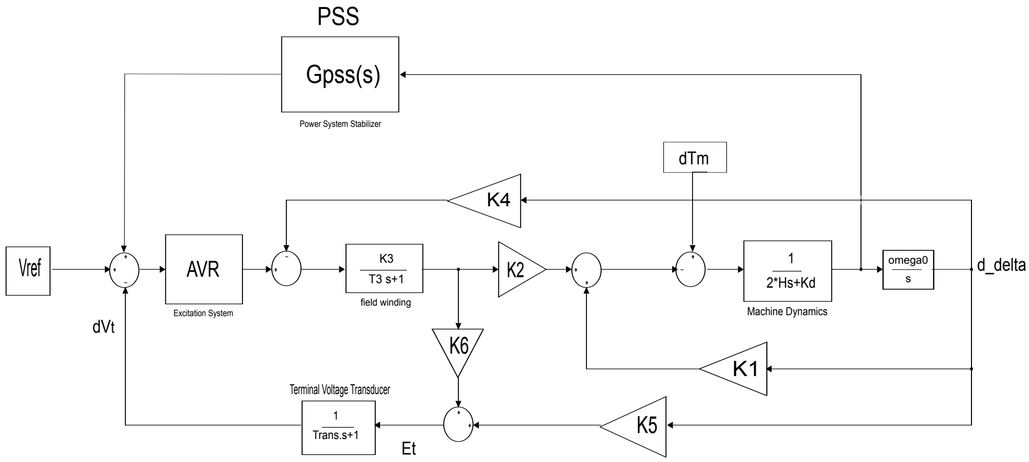

Figure 2.9: Block diagram representation of the system with PSS

The basic structure of a traditional single input PSS comprises three blocks.

- The washout filters: which are high pass filters allowing certain oscillation frequencies and eliminating steady state DC offsets [3].
- The phase compensation block: comprises of a lead-lag compensator to provide a proper phase compensation for the phase lag introduced between the AVR input and the electrical torque output [1].
- The gain of the PSS: it is set to add enough amount of damping for the compensated signal.

2.5 IEEE basic PSS model description

There are many IEEE PSS models described in [7]. The simplest model is the single input model which is PSS1A. As already mentioned in section 1, the PSS generally use speed, frequency or the power signal as stabilising signal.

PSS based on speed input is the oldest method, where the measured speed deviation from generator shaft is used as the input and it is shown in Figure 2.9 where $\Delta\omega_r$ is the speed deviation. One drawback of this is disturbance, when it is used with long shaft turbo generators, it gets affected by the torsional oscillations. Long shafts require several measurements in order to get correct value of shaft speed [14].

The second category is PSS based on frequency input. The advantage of this is that it provides better damping for inter area oscillations. This is because it is more sensitive to oscillation modes in large areas[14],[15]. The disadvantage of this method is that it is also effected by the torsional oscillations similar to the speed input. Also, the frequency derived from terminal voltage may contain noise.

For the PSS based on power input, the equation of motion of a rotor is given by the swing equation,

$$\frac{\delta\Delta\omega}{\delta t} = \frac{1}{2H}(\Delta P_m - \Delta P_e) \tag{2.16}$$

where H represents the inertia constant, $\Delta\omega$ is speed deviation, $\Delta P_m, \Delta P_e$ is change in mechanical and electrical power respectively. If the mechanical power is assumed constant then acceleration and electrical power deviation is proportional. The disadvantage is that if there is mechanical power variation, there will be unwanted output at the stabilizer[15].

2.5.1 PSS2B

The integral of accelerating power method is used to overcome problems associated with torsional oscillations and turbine power changes. PSS2B model is developed by taking into consideration the change in mechanical power and having dual input stabilizing signal. Figure 2.10 shows the block diagram of PSS2B[7].

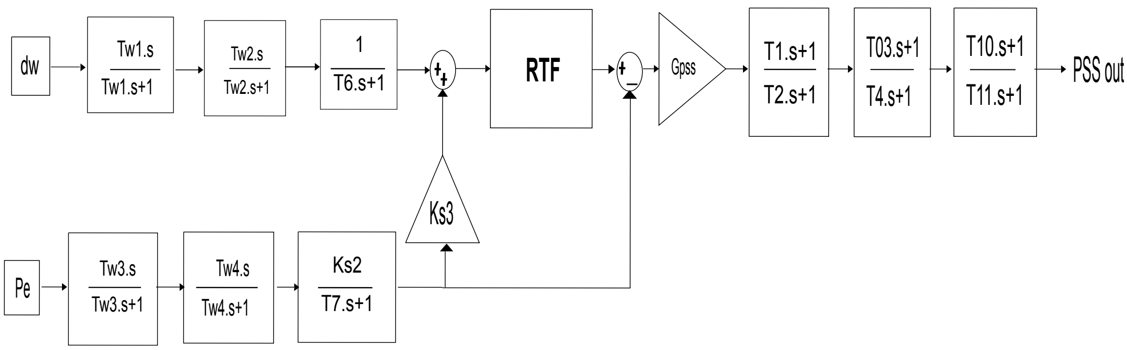

Figure 2.10: Block diagram of PSS2B

The PSS2B uses the combination of power and speed or frequency as the stabilizing signal. The first stage is the transducer. This is followed by washout filters for each input. The washout filters are high pass filters which blocks the steady speed, frequency or power signal. The signal given to the gain G_{PSS} is the synthesised speed signal or the integral of accelerating power. This is obtained with the help of the pre filter Ramp Tracking Filter (RTF).

From the equation of motion (2.16), the integral of accelerating power can be derived as [16]

$$\Delta\omega = \frac{1}{2H}\int(\Delta P_m - \Delta P_e)dt \tag{2.17}$$

To obtain the integral of accelerating power there are two terms $\frac{1}{2H}\int \Delta P_m$ and $\frac{1}{2H}\int \Delta P_e$ needed. The second term integral of electrical power is obtained easily as one input to PSS2B is power. The power is passed through the integrator block, the transfer function of which is given by [7].

$$TF = \frac{K_{s2}}{T7s+1} \tag{2.18}$$

,where $Ks2 = \frac{T_7}{2H}$. Hence the integral of electrcial power is obtained. Now (2.17) can be re-written to get integral of mechanical power

$$\int \frac{\Delta P_m}{2H}dt = \Delta\omega + \int \frac{\Delta P_e}{2H}dt \tag{2.19}$$

where $\delta\omega$ is the speed input to PSS2B. Now these signals are added and given to the RTF. The transfer function of RTF is given as:

$$F(s) = \left[\frac{1+sT_8}{(1+sT_9)^M}\right]^N \tag{2.20}$$

where, $T_8 = MT_9$. The main purpose of RTF is to track the ramp in mechanical input with minimum or zero tracking error. The signals above the corner frequency of $1/T_9$ is attenuated[3]. At the output of RTF, the integral of electrical power is subtracted from the equation (2.19) to obtain the synthesised speed. This is possible because of cancellation of ramp in electrical power at the summing junction thus removing steady state output changes due to ramp-in of power.

Finally the synthesised signal is given to the G_{PSS} and lead/lag filters to provide damping and phase compensation respectively.

3

PSS2B Tuning and Filter Implementation

3.1 Introduction

This chapter deals with tuning of PSS2B, which is done to ensure a proper operation of the PSS. An investigation is also done to implementing appropriate filter to reduce noise originating from the torque.

When tuning a PSS, one should account for the phase compensation provided by the PSS [1]. The main problem of this method is that the parameters δT_e and $\delta\Delta$ may be a little difficult to measure accurately and implement on site. This is overcome by measuring the frequency response of a signal from the AVR reference voltage to the terminal voltage output for a closed loop model, which gives good estimate of the phase compensation needed by the PSS [17].

There are several methods for tuning a PSS for SMIB system. Some of the methods described in the literature are GEP(s) method, P-Vr method, based on transfer function residue, pole placement and frequency response. As a more practical way frequency response technique is being used for analyzing and tuning the PSS. The washout filters are set to appropriate values to capture as much signal as possible in the range of frequencies of interest while eliminating offsets and steady state values. They are followed by choosing the appropriate time constants for the RTF filter. Then the phase compensation needed will be provided by lead/lag filters.
The implemented PSS along with the AVR must have a desired performance and should be able to add enough damping and preferably some synchronizing torque without affecting the stability of the whole system. The requirements or criteria for a stable system with good performance can be summarized as follows:

- Requirement for a good PSS damping: For signals measured from PSS speed input to terminal voltage, the phase of the system must be within $\pm 90^0$ and preferably near 0^0 in the PSS operating range (0.1-2.5Hz). Similarly the gain should be in the range of +20dB even though it can be set based on the SMIB stability requirements. The PSS must compensate for AVR and generator, in practice under compensation is desired to keep synchronising torque component positive.

- Requirement for PSS being stable: In order the system to be stable with the addition of the PSS,for signals taken from reference voltage to PSS output, the gain must be less than 1 when the phase is ± 180. This criterion will tell if the system meets closed loop stability with the addition of the PSS.
- Requirement for PSS suppressing turbine torque noise: In order for the PSS to be effective in suppressing the torque noise, it should have low gain as possible for frequencies in the range of torque noise. The evaluation is made using signals taken from mechanical torque to the terminal voltage or the PSS output.

These criteria are being checked after the implementation stage.

3.2 AVR tuning

The first step in tuning of the system is to ensure that it works within limits and has good performance without adding PSS. This is done by adjusting the parameters of the AVR during off line and on-line operating conditions. The simulink model given in chapter 2 in Figure 2.7, is for off-line operation of a PID type AVR with its brush-less exciter, it can also be written as transfer function.

$$AVR = (K_p + \frac{K_p}{sT_i})(\frac{1 + sT_d}{1 + s(\frac{T_d}{K_{dex}})}). \tag{3.1}$$

$$Br_{ex} = \frac{1}{1 + sT_{ex}}. \tag{3.2}$$

,where the parameters of the AVR are K_p=Proportional gain, T_i=Integral time constant, K_{dex}=Differential constant, T_d=Differential time constant and T_{ex}=Brush-less exciter time constant.

The values of the chosen parameters are given in Table 3.1 and the step response of the terminal voltage is shown in Figure 3.1. From Figure 3.1,it is clear that the system has a rise time of $0.52s$ when $Ti = 5s, Kdex = 3s$, which is a bit slow but acceptable. It can be seen that the settling time is $0.857sec$ which is a reasonable values.

Table 3.1: AVR tuning Values

Tuning Method	Parameters	Rise Time	Settling Time	Over Shoot
PID Tuning	Kp=15 Ti=5 Kdex=3 Td=0.3 Tex=0.3	0.5 seconds	0.9 sec.	Amplitude=1 Percentage=0.2%

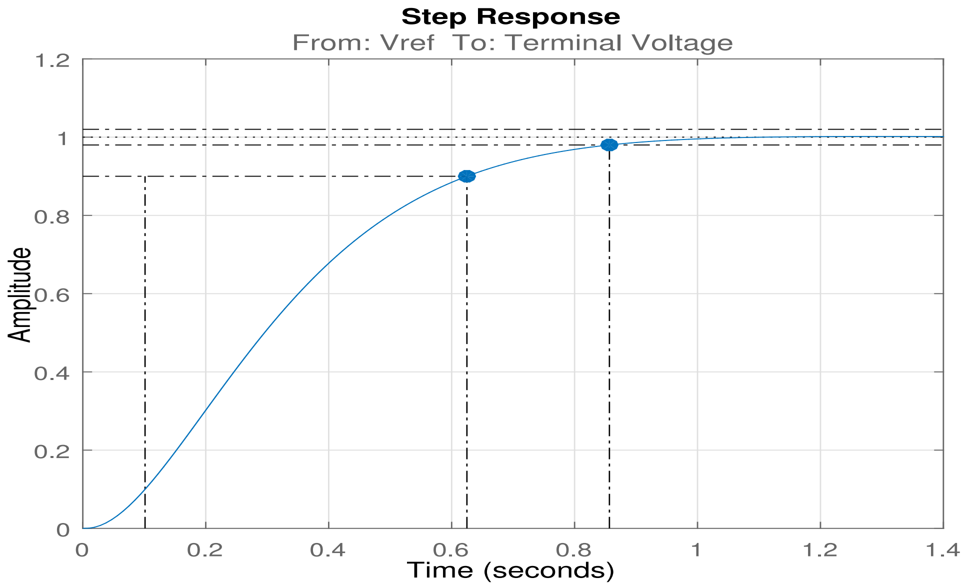

Figure 3.1: PID AVR step response

The frequency response from voltage reference to terminal voltage is already plotted in chapter 2 in Figure 2.8. The response corresponds to an AVR response when the generator is not connected to the grid.

AVR performance during generator on-line operation

In this setup, generator is connected to the grid, thus referring to the block diagram explained in Figure 2.6 without PSS.

The bode plot from voltage reference to terminal voltage is shown in Figure 3.2. The operating conditions used for the calculations are shown in Table 3.2. The operating condition 1 shows the lowest loading of the generator with the active power is 0.6pu and highest loading is the operating condition 4, where the active power is 0.9pu.

The values of the linearized model parameters (constants) in Table 3.2 are calculated using equations derived in Chapter 2,more information can be also be in the appendix

A. Only the two extreme conditions of the machine operation is plotted. This is because the system is more likely to be unstable during high loading conditions.

Table 3.2: operating conditions and respective model parameters

Operating cond.	P(pu)	Q (pu)	$X_e(pu)$	$U_B(pu)$	$\theta(pu)$	K_1	K_2	K_3	K_4	K_5	K_6
1	0.6000	0.0684	0.075+j0.713	1.000	25	0.7883	0.8282	0.5487	0.5385	-0.0327	0.7313
2	0.7132	0.1130			30	0.7790	0.9365	0.5487	0.6178	-0.0513	0.7201
3	0.8221	0.1673			35	0.7566	1.0262	0.5487	0.6821	-0.0725	0.7095
4	0.9259	0.2309			40	0.7197	1.0985	0.5487	0.7324	-0.0954	0.7000

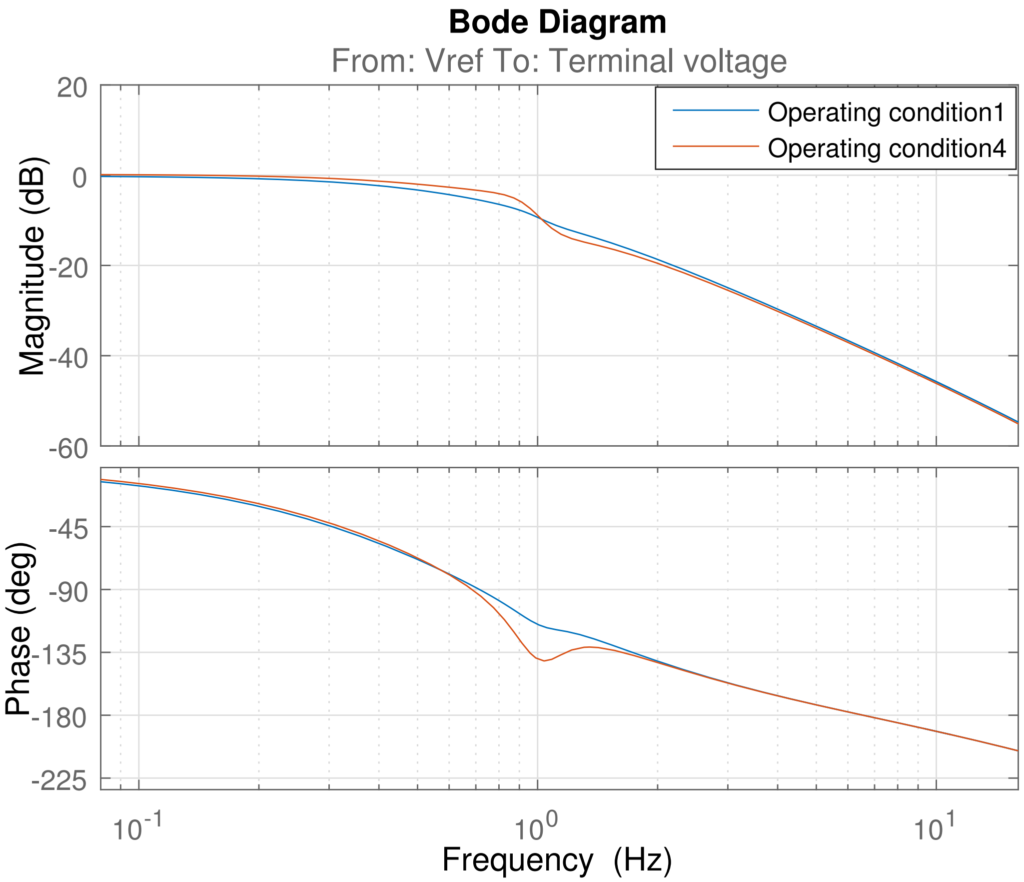

Figure 3.2: PID AVR bode plot

Figure 3.2 shows the frequency response of the AVR and the generator at the two machine loading conditions taken into account. The system has more phase lag at local mode of oscillation when the loading is at the peak which is an expected result. The overall design of the AVR and generator is in the range of acceptable limit.

3.2.1 Eigen Value Analysis

The eigen value analysis is used to predict the stability of a system. The eigen value denoted by λ can be real or complex number. The characteristics for a real eigenvalue is a non-oscillatory mode. If this real value σ is positive it implies instability. A negative real value implies stable operation.

A complex eigenvalue represent the oscillatory mode of the system. They occur as conjugate pairs in the form $\lambda = \sigma \pm j\omega$ [1]. The frequency of oscillation f can be found from the imaginary term ω and the also the damping ratio ζ can be found. The damping ratio determines how the system will respond.

$$f = \frac{\omega}{2\pi} \tag{3.3}$$

$$\zeta = \frac{-\sigma}{\sqrt[2]{\sigma^2 + \omega^2}} \tag{3.4}$$

Table 3.3: Eigen values of AVR + Genrator

Operating conditions	Eigen value	Damping
1	-1.27±1.02	0.199
2	-1.15±0.95	0.193

From the eigenvalue analysis performed for the AVR model, Table 3.3 illustrates how the result looks like for different loading conditions. The system is stable if all the eigenvalues are located on the left half of the s-plane. If the imaginary parts are very small in comparison to their corresponding real parts, then there is essentially no oscillation. In any eigenvalue analysis, the greater the negative value of real part, the greater the systems oscillation gets damped [18]. The result of the bode diagram for the AVR and generator are similar to the results shown in the table.Hence in order to increase the damping of the oscillations at these frequencies, it is important to tune the PSS at these modes. This will allow the system eigenvalues to shift to the left, with addition of more PSS gain.

3.3 PSS2B tuning, performance requirements

In this section, the reciprocating engine torque noise is studied first, this helps to find the dominant frequencies. Later, the various components will be tuned for proper functioning of PSS2B while at the same time ensuring the PSS is not sensitive to torque noises.

3.4 Case study: Reciprocating engine noise

Torque noise created from reciprocating engine may cause PSS saturation or saturation of AVRs due to their high gain at high frequencies[17]. There are papers investigating application of torsional filters in order to get rid of these higher frequency noises or oscillations. However implementation of these filter has its own disadvantage that they introduce additional phase lag at operating frequencies (lower frequencies) that can distort the operation of the PSS which is tuned for lower frequency of machine modes of oscillation [19]. This implies that it can limit the amount of gain provided by the PSS[1].

Different real time measurement data obtained from Wärtsillä shows the effect of the torque noise originating from a reciprocating engine. The data measurements were taken when the PSS is on and when the PSS is off. A Fourier transform analysis (FFT) is performed in order to study the noise behavior and trace dominant frequencies of the noise signal, which can be seen in Figures 3.3 to 3.8, below. The real time measurement data such as the PSS frequency input, PSS power input and PSS output signal are studied.

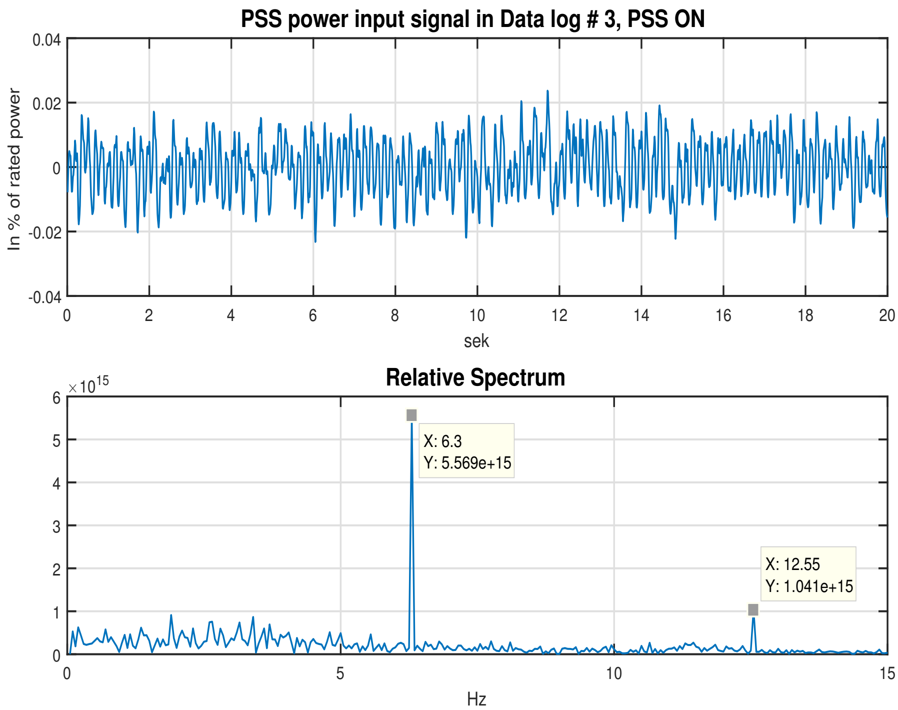

Figure 3.3: PSS2B power input

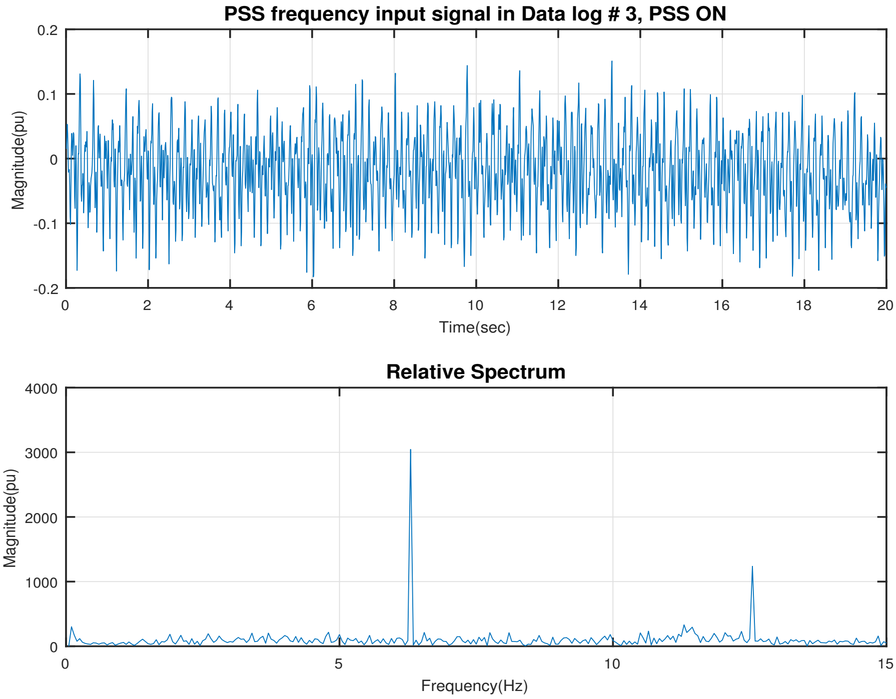

Figure 3.4: FFT: PSS frequency input

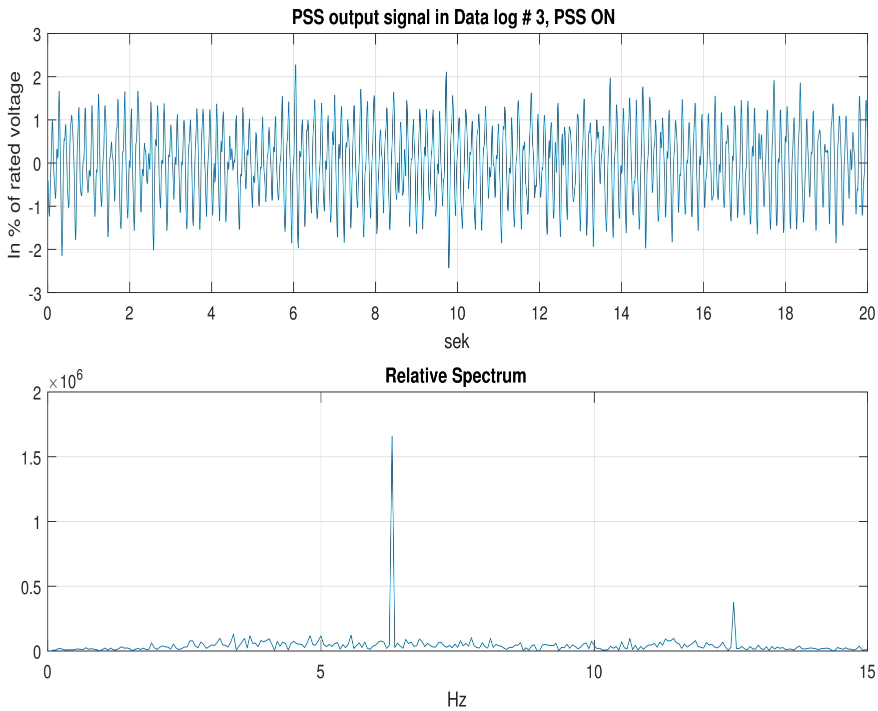

Figure 3.5: FFT of PSS output signal when the PSS is ON

The plots given in Figures 3.3 to 3.5 show several real time measurement data provided when the PSS is ON. Figure 3.4 shows frequency input of the PSS at the time when the PSS is connected to the AVR. It can be clearly seen from the FFT plot that the dominant frequencies of the noise signal occur at 6.3Hz and 12.55Hz. It is also obvious that other noise component frequencies are present with low power. The signal measurements when the PSS is off are plotted in Figures 3.6 to 3.8.

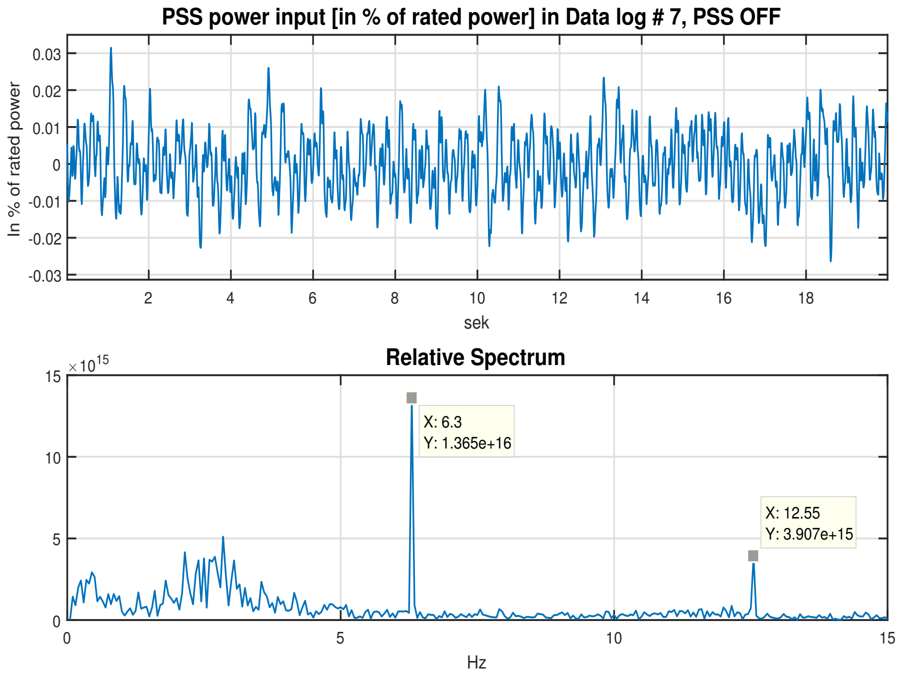

Figure 3.6: PSS2B power input

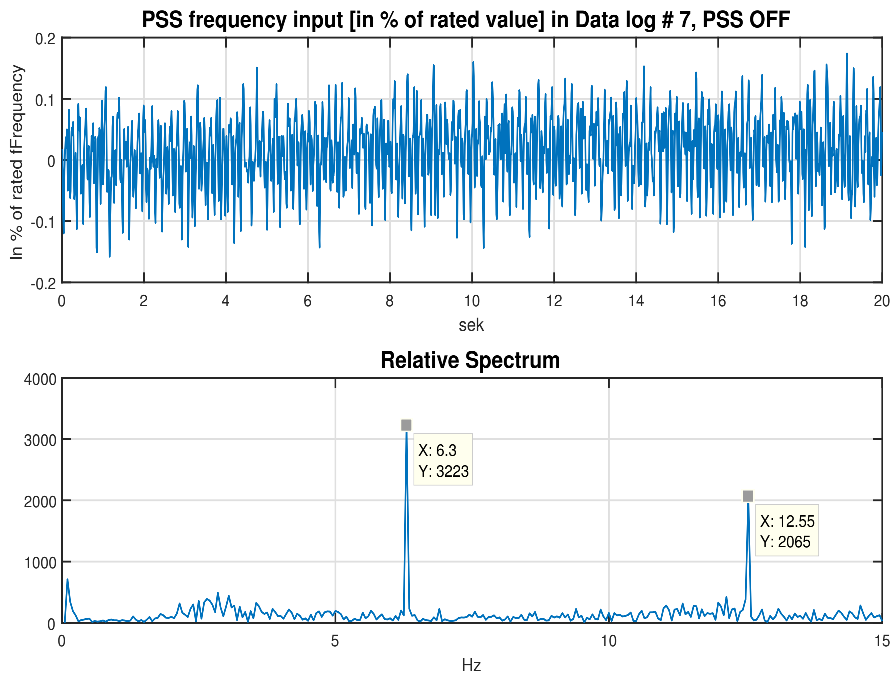

Figure 3.7: FFT: PSS frequency input

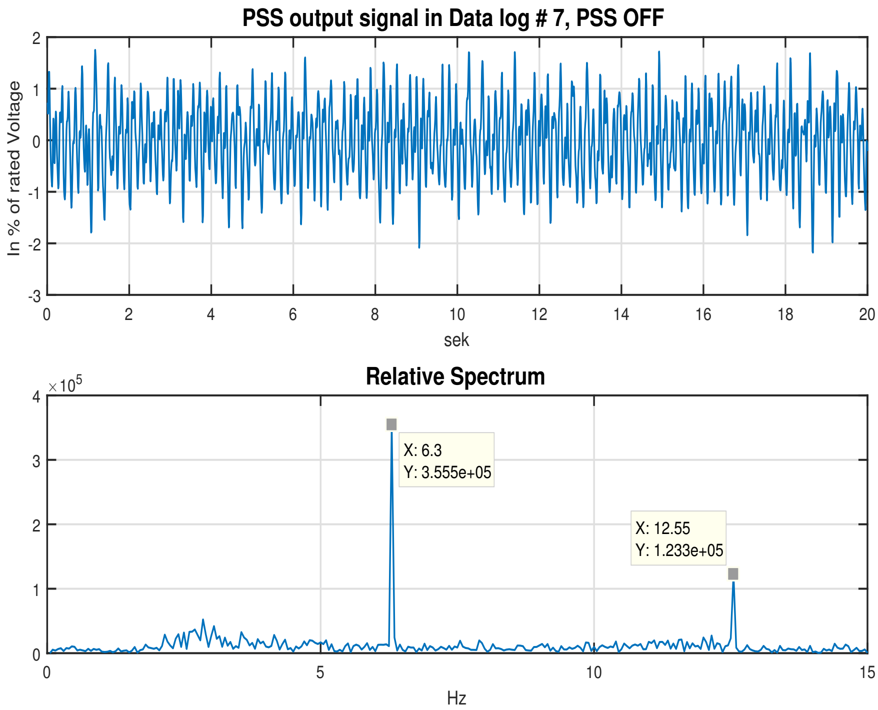

Figure 3.8: FFT of PSS output signal when the PSS is OFF

Torque noise extraction

In order to have a clearer information on the incoming noise from the reciprocating engine and simplify the difficulty in real time measuring the mechanical noise, it is mathematically extracted from the available measurements. This is done using swing equation.

$$\Delta\omega = \frac{1}{2H}\int_0^t (\Delta P_m - \Delta P_e)dt; \tag{3.5}$$

,Where t referes to the time in seconds which ranges from $t = 0 \rightarrow 20$ seconds. Equation (3.5) gives mathematical relationship between mechanical power input, electrical power input and rotor speed. The result of the simulation is plotted in Figure 3.9. The torque noise FFT is not affected whether the PSS is on or off, hence extraction is done from the PSS on data measurements. To get the mechanical power, (3.5) is being transformed to Laplace domain and rearranged

$$\Delta P_m = 2Hs\Delta\omega + \Delta P_e \tag{3.6}$$

The parameters of the mathematical relationship derived in (3.6) are: ΔP_m mechanical power or torque perturbations, $\Delta\omega$ rotor speed perturbations and ΔP_e electrical power or torque perturbations

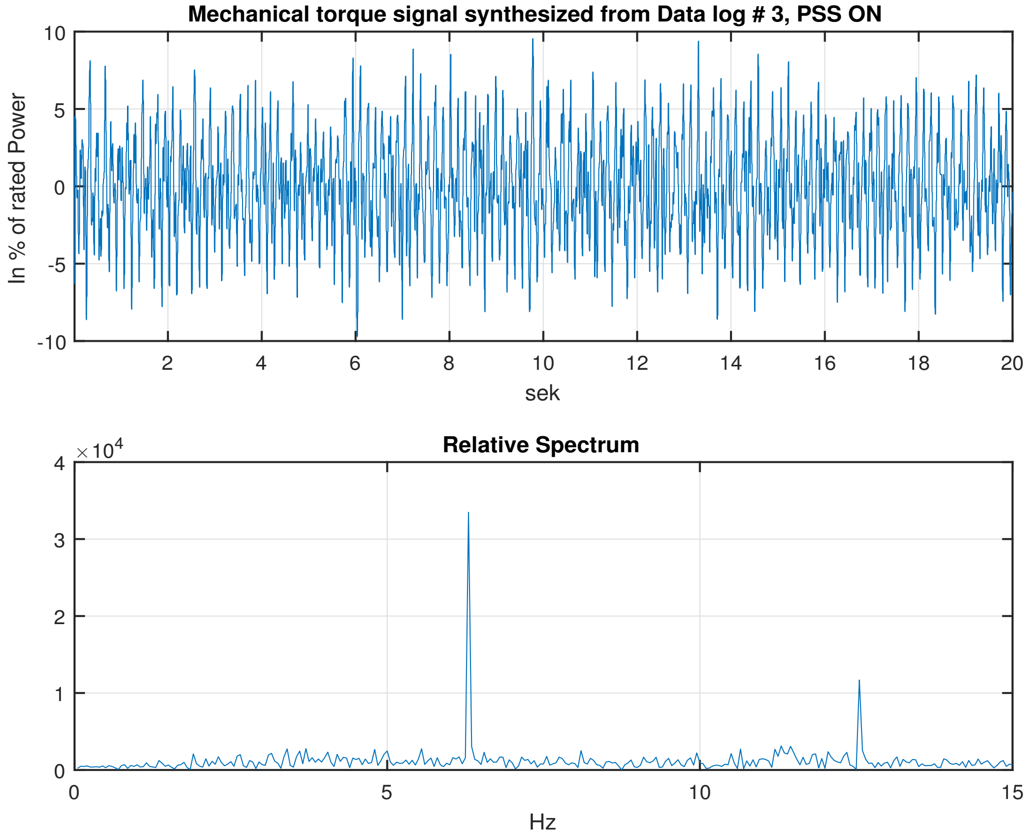

Figure 3.9: Time domain signal of Synthesized torque Noise and an FFT signal that indicates where the dominant frequencies are located

Figure 3.9 shows the synthesized torque noise using (3.6). It is found that the FFT of the signals when the PSS is on and off proves that the dominant frequencies that originate from the reciprocating engine are the same. Those frequencies detected are at 6.3Hz and 12.55 Hz.

3.5 Washout Filters and signal transducers

The transfer function of a transducer is given as

$$Trans(s) = \frac{1}{1 + st_r} \tag{3.7}$$

,where t_r represents signal transducers time constant usually in the range of milliseconds. In this design consideration t_r=0.006s is taken.

One of the important tuning procedure of a PSS is determining the washout filter time constant. The main purpose of the washout filters is to suppress steady state offset of the input signal and to attenuate signals of frequencies lower than electromechanical modes of oscillations (less than 0.1 Hz). The transfer function is given as:

$$Wo = \frac{T_w}{1 + sT_w} \tag{3.8}$$

,where T_w refers to the washout time constant in seconds.

(3.8) is used for a single washout filter. Investigation of washout filter frequency and time response as plotted in Figures 3.10 and 3.11 show that using two washout filters has several merits over using one washout filter [3] because it:

- Improves response of ramp input in electrical power to prevent generator terminal voltage offset as well as reactive power output.
- Provides a greater flexibility of reducing the time constant of each washout filter thus improving the time domain performance by the washout filters, even though the washout filter time constant greatly depends on the modes of oscillation of interest.

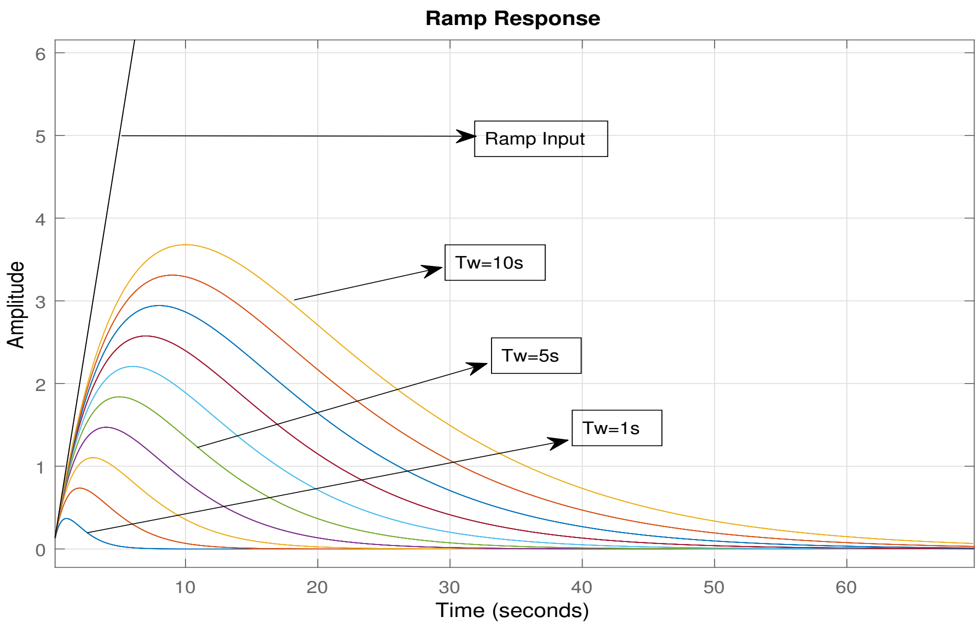

Figure 3.10: Two Washout filter Ramp response

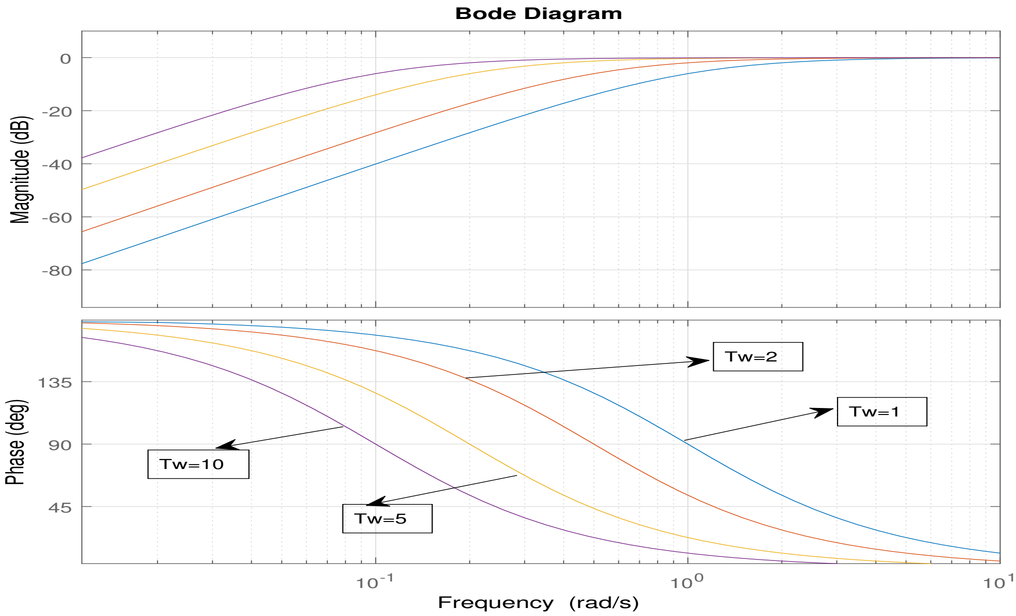

Figure 3.11: Bode diagram of two Washout filters in series

Figure 3.10 shows the ramp response of the two filters. As can be observed from the bode plot diagram of the two washout filters in series in Figure 3.11, the phase lead introduced increases with decreasing time constant. The time constant of 5 seconds is the proper value that gives a phase lead of around 30^o around 0.1Hz of oscillation frequency.

3.5.1 Ramp Tracking Filters

The next step in tuning a PSS involves the proper design of RTF filters inside the PSS2B by identifying or choosing appropriate time constants.

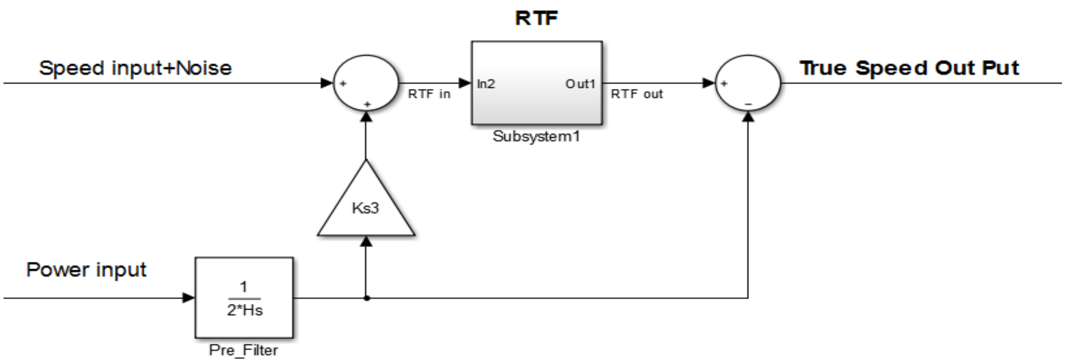

Figure 3.12: PSS2B used for RTF investigation

As can be seen from the Figure 3.12, a perfectly synthesized speed signal is assumed to be obtained from power input using the swing equation (3.5). The bode plot of Figure 3.13 shows the ideal working of RTF by passing the signal without an additional gain and phase which is indicated by the yellow line. This implies the time constants are chosen such the RTF selects the best signal that truly represents the speed signal. Keeping the primary purpose of the RTF in tracking the ramp input signal with minimum tracking error [3], it has a greater influence in attenuating the signals with frequencies above $\frac{1}{T_9}$. This means the corner frequency of the RTF is determined mainly by the value of T_9 which was explained in section 2.5.1.

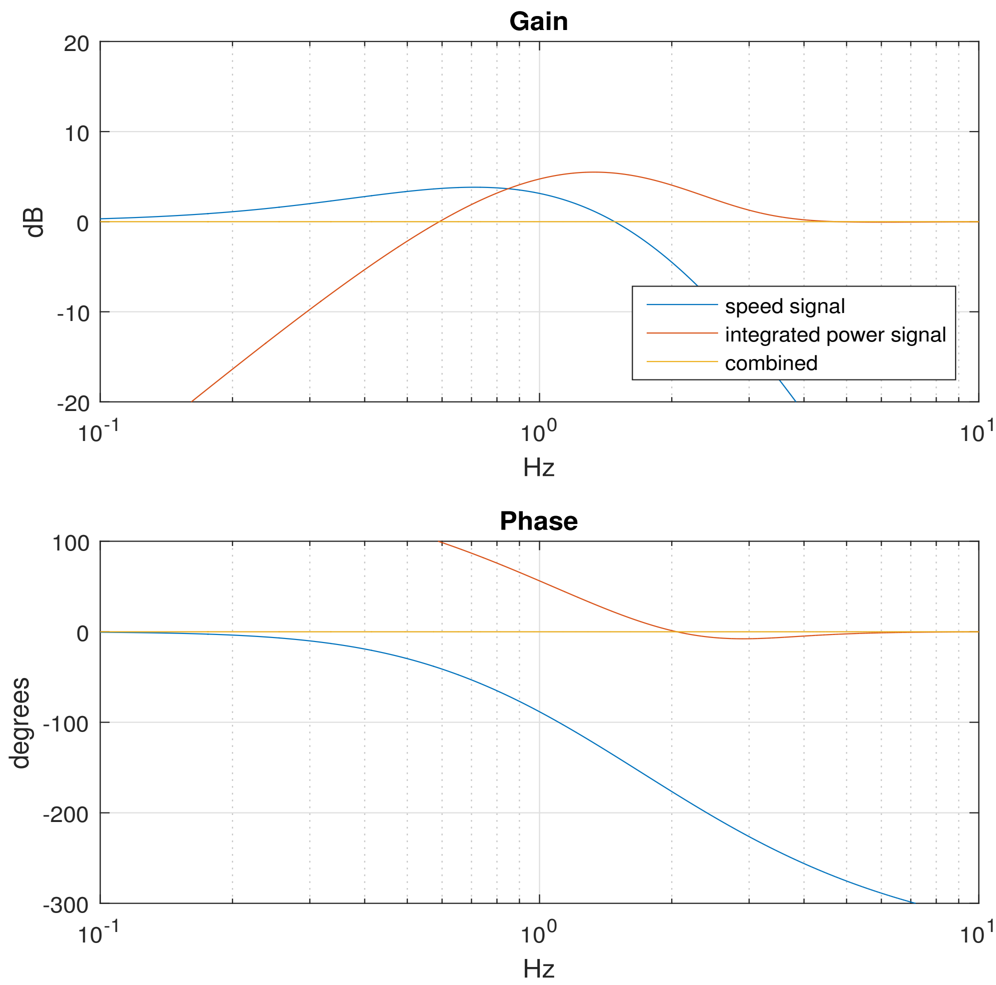

Figure 3.13: General Ramp Track frequency response

Effect of RTF on system

Different values of time constants T_9 are tried considering speed input and later considering power input only. The values taken into account for investigation are being put in table 3.4. Here N value is chosen as 1, in order to study the property of one RTF filter.

Table 3.4: RTF tuning

Selection	T_9	M	N	$T_8 = M.T_9$	Comment
1	0.0001	5	1	0.0005	Speed only
2	0.1	5	1	0.5	Normal
3	10	5	1	50	Power only

The linearized SMIB model with mechanical torque noise is investigated for different RTF time constants. The frequency response is taken from mechanical torque to PSS output as shown in Figure 3.14. The requirement for the PSS to suppress the noise effectively is that, the gain of the system should be as low as possible in the frequency range where torque noise typically occurs, which is near 10 Hz for this case study.

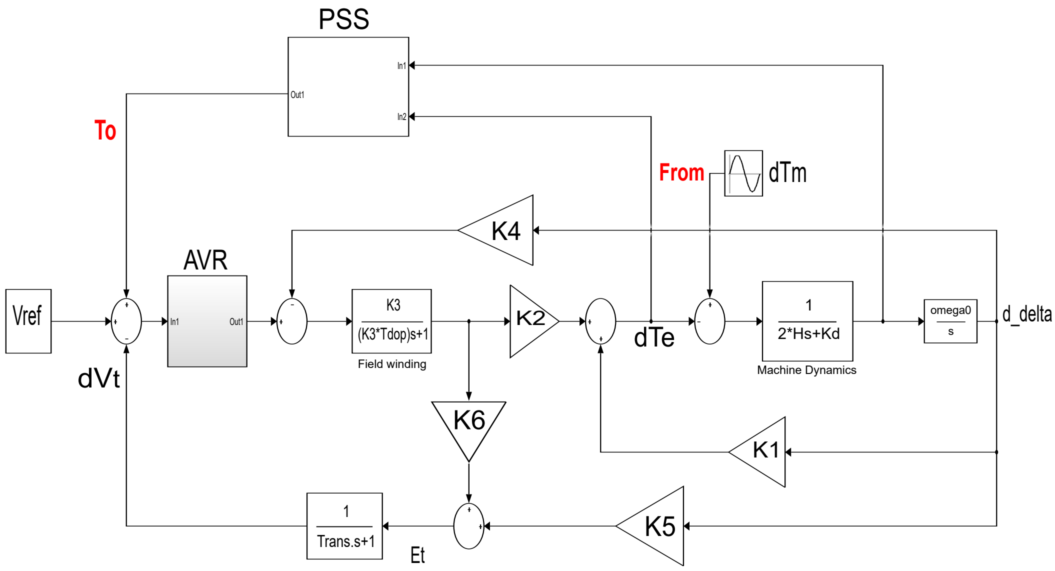

Figure 3.14: SMIB model of PSS block diagram with mechanical torque variation

Figure 3.15 is plotted with three different time constants for the RTF filter. The RTF cut-off frequency at $T_9 = 0.0001$, indicates that PSS is serving as a speed input only. For this type of PSS, there is good damping for the low frequencies but is susceptible for high frequencies. When time constant is set to a high value, that is $T9 = 10$ it can be considered as power input only. Here the system is susceptible for low frequency noise while the high frequency noise is greatly attenuated due to the integrator of the power signal, which increases the roll off even faster thus increasing the overall attenuation at higher frequencies indicated by the yellow line in Figure 3.15. Therefore the combined speed and power input, that is the typical PSS2B performance is achieved by time constant value of $T9 = 0.1$. It is observed that the damping in both the low frequency and high frequency range has been achieved as compared to single input PSS.

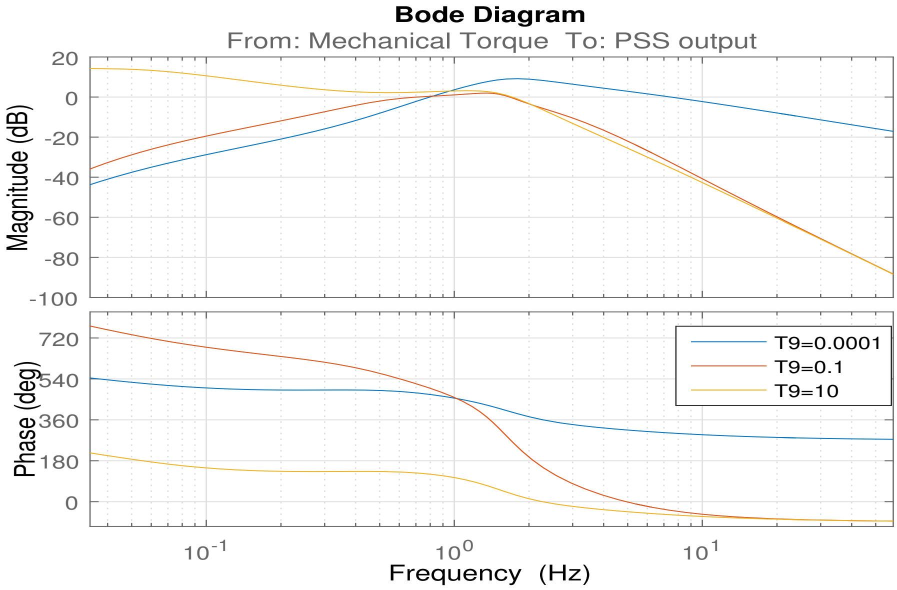

Figure 3.15: Bode plot for signals taken from mechanical torque to PSS output

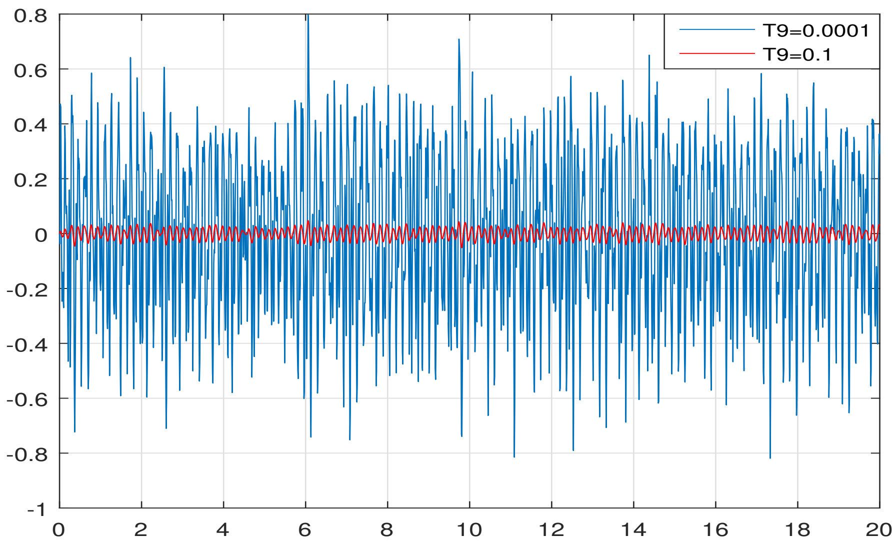

Figure 3.16: PSS time domain output for speed only and normal ramptrack filter

The time domain plot 3.16 shows the PSS output for different RTF cutoff, with synthesised torque noise injected. The result shows that the high frequency noise has been attenuated more with PSS2B than the speed only input.

The above investigation gives a clear understanding in choosing the right parameters for the above RTF filter. The value of T_9 around 0.1 is found to be adequate to fulfill the appropriate cut-off frequency of around 3 Hz. This allows the RTF filter to choose the best signal that corresponds to the true speed signal.

3.6 Lead-Lag filters

For the PSS to function as designed (which is to enhance the SMIB system damping torque and to some extent synchronizing torque), the phase lag introduced by the AVR and the exciter must be compensated. This is to ensure that the torque component produced by the PSS is in phase with the speed signal. The usual procedure in lead-lag filter tuning procedure includes calculating the eigenvalues to identify the dominant modes of oscillation. An alternative and more practical way is study the phase lag introduced in the frequency response of the system from reference voltage to the terminal voltage without the PSS being included.

The more the phase lag the more is the compensation needed, which in-turn increases the gain of the whole system at higher frequencies thus degrading the performance of the filters implemented. Therefore, care should be taken in choosing lead-lag filters time constants. Due to that, the primary task is to analyse the amount of phase lag introduced by the AVR and generator.

From the phase response of Figure 3.2, the lead-lag filters are used in-order to compensate the phase lag and make it closer to zero or at least within 90 degrees in the PSS operating frequency range.

The transfer function of a lead-lag filter is given by

$$TF(s) = \left[\frac{1 + T_1 s}{1 + T_2 s}\right]^n \tag{3.9}$$

, where T_1 and T_2 are the time constant of the filter and n represents the order of the filter.

With the proper values of time constants the bode diagram of the compensating filters is shown in Figure 3.17 with a maximum phase that lies at around the local modes. For filter L1, the values used for T1 and T2 are 0.17 and 0.02 sec respectively. Similarly, the combined phase of filters that were used is around 90 degrees. The values of time constants are given in appendix B.

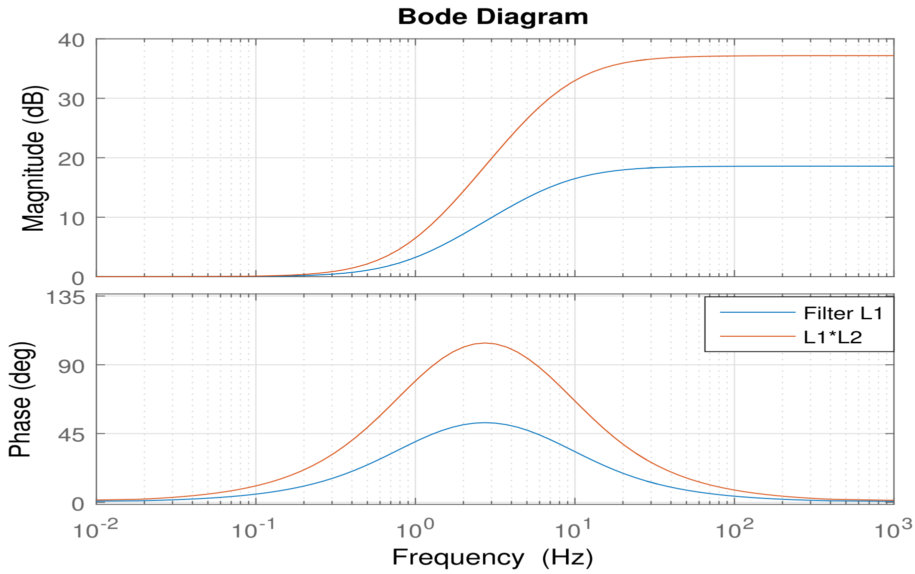

Figure 3.17: Lead-Lag filters bode diagram showing individual as well as combined phase and gain behaviour

3.6.1 Gain Tuning

As per [1], the gain is increased to improve the damping of oscillations until the system is in stable operation. A closed loop control system including a PSS can have several modes of oscillation. Usually the local modes of oscillation, where the machines oscillates against the infinite bus, is taken into consideration for tuning purposes.

Most of the time and more traditionally, the gain of the PSS is set as one third of the value as an maximum operating gain beyond which the system has a tendency to go unstable. This method is used here to set the gain. This method is chosen due to the difficulty of obtaining the root locus or the eigenvalues of a complex system on site [1]. By setting it to one third of the value a gain margin of about 10 dB is provided. Usually the gain of a PSS varies from 10 to 30 depending on the amount of damping needed. Here, a value of 20 is chosen. All the values of PSS2B taken into consideration is listed in appendix B.

3.7 Notch filter design

Several papers have investigated the use of low pass filters to reduce mechanical noise, but only for the purpose of reducing torsional noise originating from turbine shaft oscillations. In this scenario, the noise origin is from the reciprocating engine torque itself. In order to specifically remove the dominant torque noise frequencies, introduction of notch filter with a carefully selected centre frequency can be a good choice without greatly affecting the phase of the system in the total control loop. When a band reject or notch filter is being added in the control loop of the PSS, the filter should be able to attenuate torque noises with minimum phase lag in the system [17].

There is always limitation to the extent of attenuation the notch filters can provide. It would be ideal to introduce a notch filter with very high attenuation. In the contrary, the phase lag introduced by the filters would add with the phase lag from the AVR input till the electrical power input. This situation would demand a much more phase compensating filters for the PSS to provide proper damping. The gain of the lead-lag filters in the control loop would increase thus reducing the amount of gain that we can add. This can also have a deteriorating effect on noise reduction at higher frequencies.

3.7.1 Investigating effect of different filters on PSS and System stability

For choosing the appropriate filter size, different notch filters, as shown in Table 3.5 are investigated. Notch filters of different depth and band-width are taken into account. In Table 3.5 different notch filters with different centre frequency, including at 6Hz and one notch filter of centre frequency at 12Hz are shown, since the noise extracted was found at these frequencies. The rest of the notch filters and their specifications are given in the Appendix C. The PSS parameters taken for the investigation is given in the Appendix B.

The system with PSS2B, AVR and generator in combination is simulated with one filter included at a time. The gain margin (GM) and phase margin (PM) of the system is taken during full load, measured from reference voltage to PSS output for open loop condition. The phase of the system at 2Hz is studied by measuring the signal from PSS speed input (or, more precisely, from combined speed and power input, with power derived from speed) to terminal voltage. The noise damping (given in dB) and RMS ratio (normalized with respect to No Notch case) is taken for the closed loop system with PSS by comparing the PSS output signal and the mechanical torque noise.

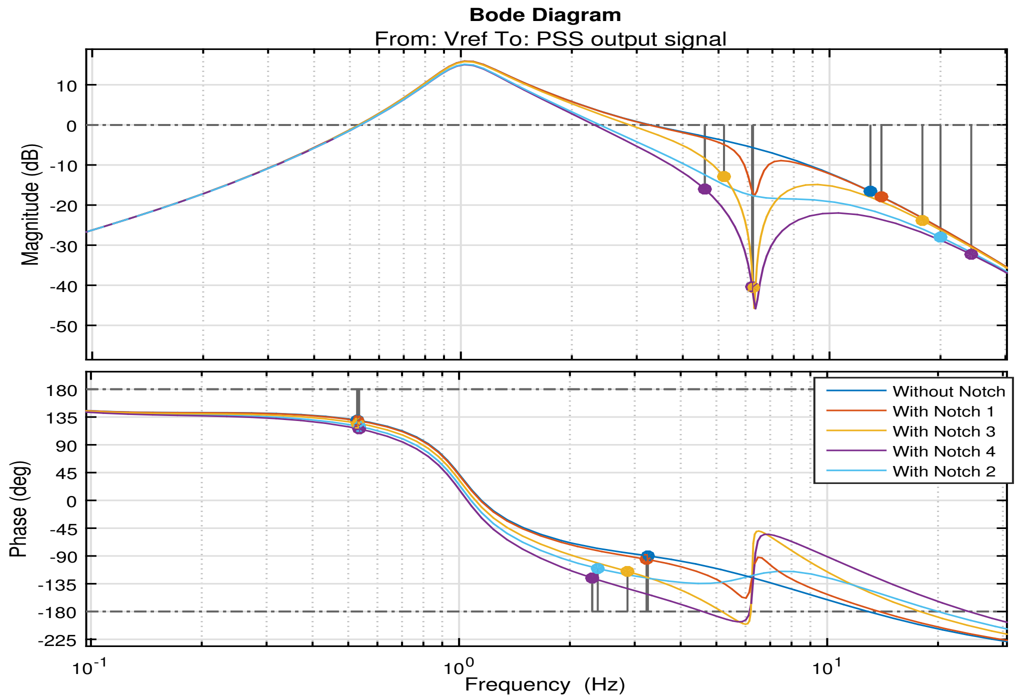

Figure 3.18: Bode plot for signal taken from Reference voltage to PSS2B output for the investigation of different Notch filters

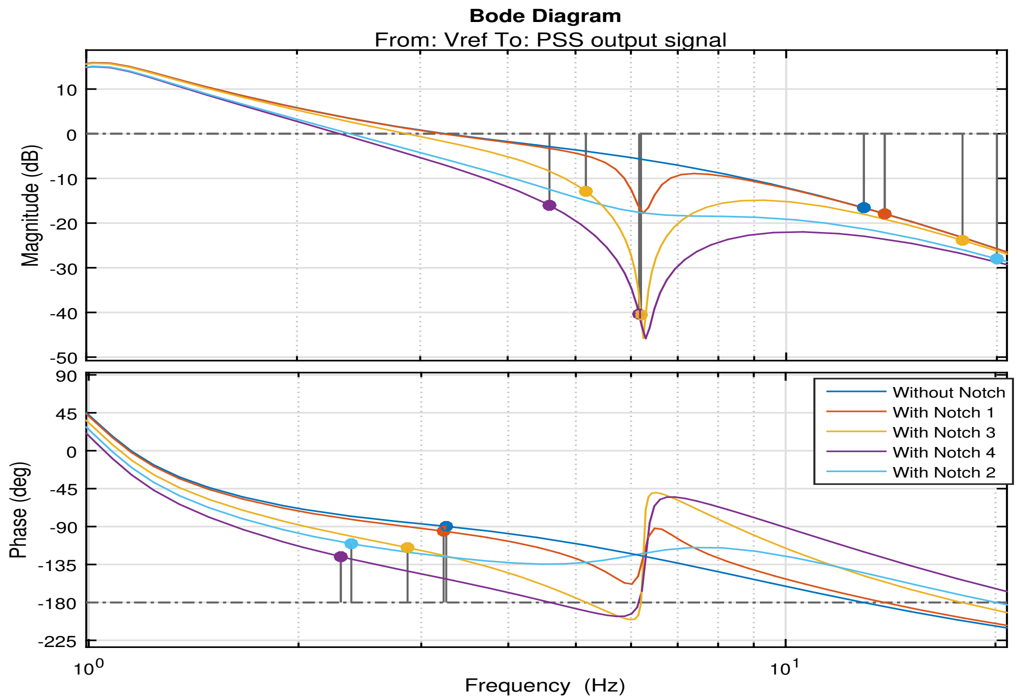

Figure 3.19: Bode plot of the system from Voltage reference to PSS2B output terminal, zoomed closer to the notch

Figure 3.19 is a closer view of Figure 3.18. It is observed from Figure 3.18 that, as the notch size increases the gain margin increases. Similarly, the phase margin gets closer to -180^0 which means closer to instability point.

Table 3.5: Selected notch filters with stability margins

Notch	Depth (dB)	Width (Hz)	PM (deg)	GM (dB)	Attenuation (dB)	RMS ratio normalized around No notch	Phase 2 Hz
No notch			90.2	16.6	0.61	1.000	4
3a	-12	1.18	84.5	17.9	10.9	1.064	9.8
6a	-12	6	73	22.3	12.35	0.903	0.9
8a	-12	14.6	69.6	28	14	0.745	-14.8
3b	-17	1.18	84	18	11.7	0.976	9.6
10b	-17	15	63	29.1	14.1	0.741	-20.5
3c	-23	1.18	83.5	13.5	11.2	0.961	9.3
13c	-23	15	59	29.9	14.2	0.730	-23.4
1d	-4	6	83.5	19.7	7.3	1.614	6.2
12d	-40	6	65.8	12.7	12.8	0.850	-5.7
1e	-4	9	83.2	20.8	7.4	1.589	3.7
13e	-40	9	60.4	13.8	12.9	0.842	-13.6
1f	-4	12	83.8	21.6	8.4	1.539	1.8
13f	-40	12	57.3	14.6	13.6	0.787	-20.9
3a+12.55Hz			83.8	16.7	10.91	0.993	9.8

The results of the system response from Table 3.5 and the tables given in Appendix C are plotted in Figure 3.20. The investigation was conducted first with constant depth (of -12dB, -17dB, -23dB) and varying width. Then with constant width (of 6Hz, 9Hz, 12Hz) and varying depth.

The investigation showed that with an increase in width of the filters (depth of the notch filters kept constant), the system GM increases while the PM goes down. The noise attenuation level increase as the width increases. Similarly an investigation performed for constant width shows the GM of the system varied only slightly until the depth is 23dB and then starts decreasing. Meanwhile the PM decreases with increase in depth in similar fashion as in the previous case. It is noticed during the investigation that, the attenuation increases until the depth reaches 23 dB. Further increase in the notch filter depth above 23dB didn't show significant changes in the attenuation level.

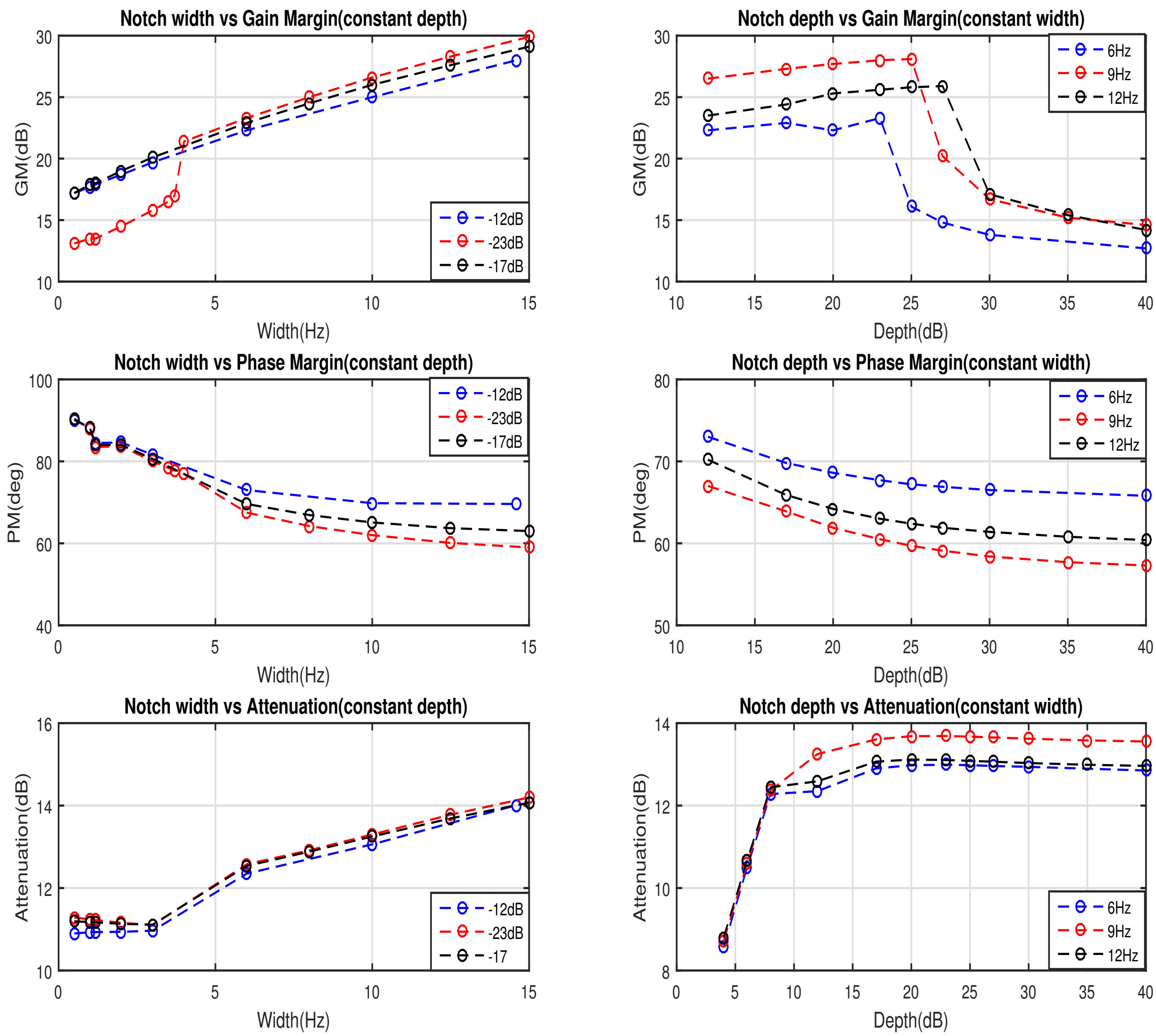

Figure 3.20: System behavior for different notch filters (a) left figure shows for constant depth (b) right figure shows for constant width

The conclusions that can be made from the investigation is that if the notch filter is very wide or very deep (eg: 8a, 10b, 13c etc from table 3.5) then PM is reduced and also the phase compensation needed at 2 Hz is higher. The good point is that GM is higher as well as attenuation. So, it is a compromise between all these factors that needs to be considered for a good design.

For choosing a depth, varying depth (constant width Figure 3.20 (b)) investigation is taken. The GM remains almost same until -23dB and attenuation varies very slightly when depth is above -9dB. Taking these into consideration, a depth of -12dB is chosen to be enough for this work. For choosing the width, Figure 3.20 (a) is taken into account. The attenuation increases after 4Hz only but the PM decreases after 4Hz. Therefore, two filters from Table 3.5 are considered, notch filter 3a (which is below 4Hz width) and notch filter 6a (which is above 4Hz width). With respect to the case without notch filter, the attenuation is increased around 12 percent while the PM is decreased by 36 percent. So a width of 1.18Hz is chosen. Therefore at typical noise frequencies of 6.3 Hz, notch filter 3a is preferred.

In situations where finding the exact locations of dominant noise frequencies is difficult, it is recommended to use notch filter 8a, since it covers a wider band of frequencies. For the 12.55 Hz noise component, a notch filter similar to notch 3a but with a lower depth (-4dB) is being used. This is because the noise at 12.55 Hz is already found to be very less compared to the noise occurring at 6.3 Hz

3.7.2 Filters Implemented

The appropriate notch filters that are being chosen to fulfill the above requirements are 3a for 6.3 Hz and transfer function given in (3.10) and for 12.55Hz the transfer function is given in (3.11). The Bode plots of the designed filters are shown in Figure 3.21.

$$H(s) = \frac{0.0006484s^2 + 0.0013s + 1}{0.0006484s^2 + 0.0051s + 1} \tag{3.10}$$

$$H(s) = \frac{0.0001608s^2 + 0.001s + 1}{0.0001608s^2 + 0.0016s + 1} \tag{3.11}$$

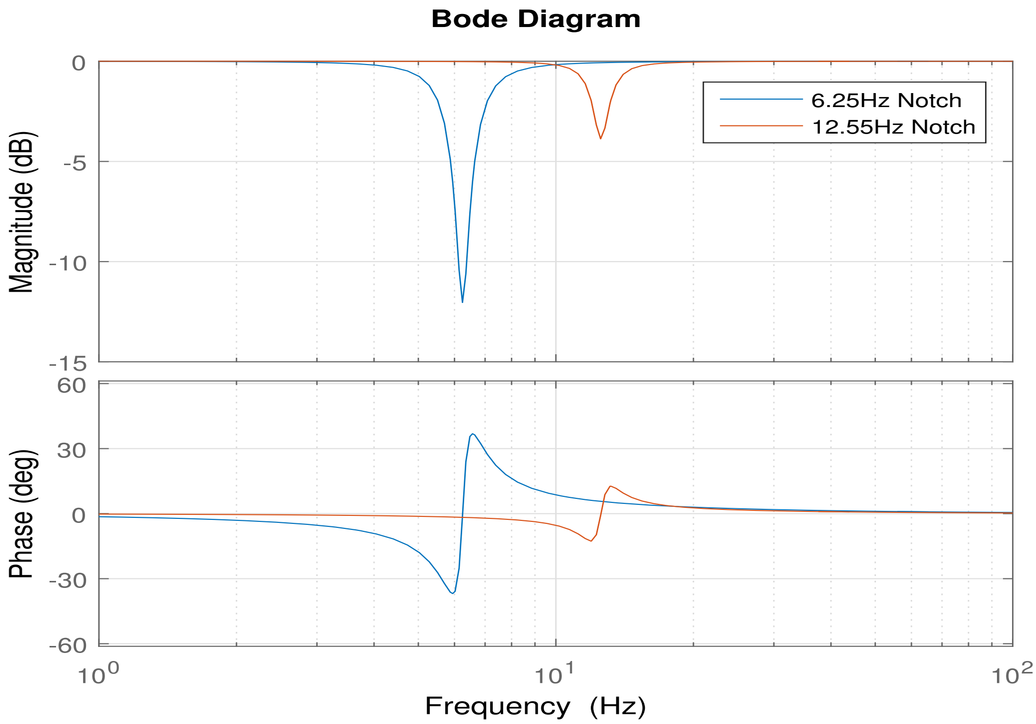

Figure 3.21: Bode diagram of two notch filters with center frequency at 6.3 Hz and at 12.55 Hz

After implementing the Notch filters designed previously in the PSS control loop, the system is being simulated by injecting the synthesized torque noise. The result is plotted in Figure 3.22 is the output of the PSS after Notch filter implementation. It can be compared with the Figure 3.5 showing the output of PSS before adding the filter. The notch filters have managed to remove the dominant noise frequency components from the system to a much lower value than before.

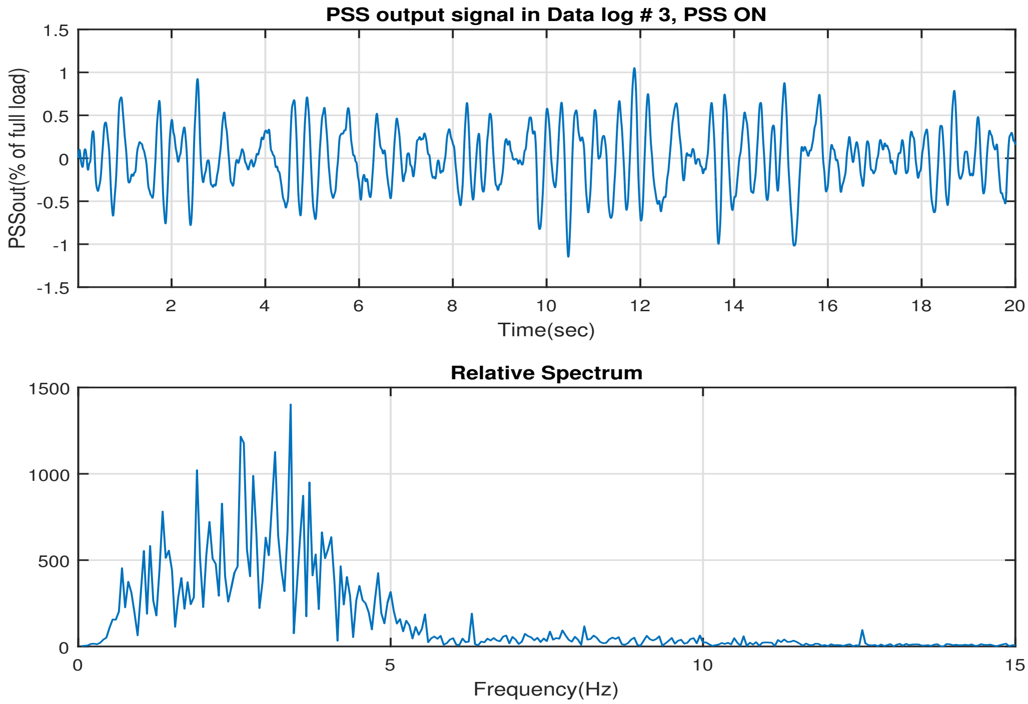

Figure 3.22: PSS output signal after inserting two notch filters

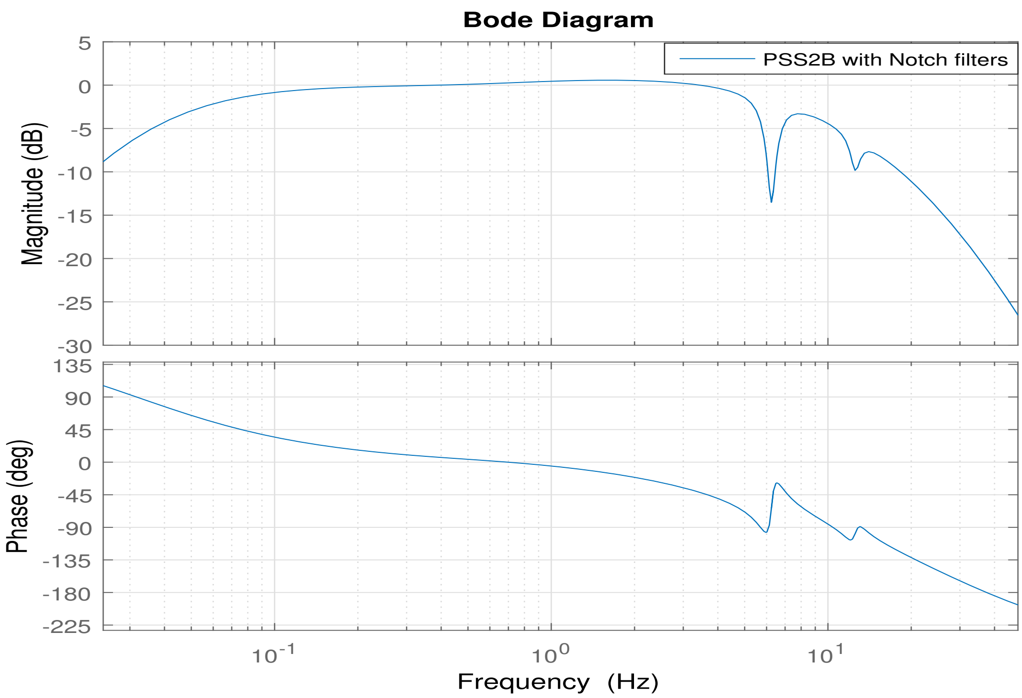

Figure 3.23: Frequency response of PSS2B taken from PSS2B speed input terminal to PSS2B output with two notch filters

The final Bode diagram in Figure 3.23 show the frequency response result after adding the notch filter transfer function of the PSS control loop. The measurement is taken from combined speed and power input, with power derived from speed as per (3.6), to PSS output. It can be observed that the two Notch filters has added to the existing attenuation level provided by the PSS.

3.8 Analysis of PSS performance criteria

The criteria mentioned in section 3.1 for the SMIB system is analysed here. These criteria are chosen such that the parameters and signal ports can be easily measured.

3.8.1 PSS Oscillation damping performance

In order to analyze the oscillation damping performance of the PSS, the frequency response plot considered from the combined PSS speed and power input, with power derived from speed, to the terminal voltage as shown in Figure 3.24 and the Bode diagram 3.25. Firstly, in 3.25 (a) without notch during offline condition when generator is disconnected from the grid and on-line (which is the high load condition 3.6). Secondly, in Figure 3.25 (b) with notch filters.

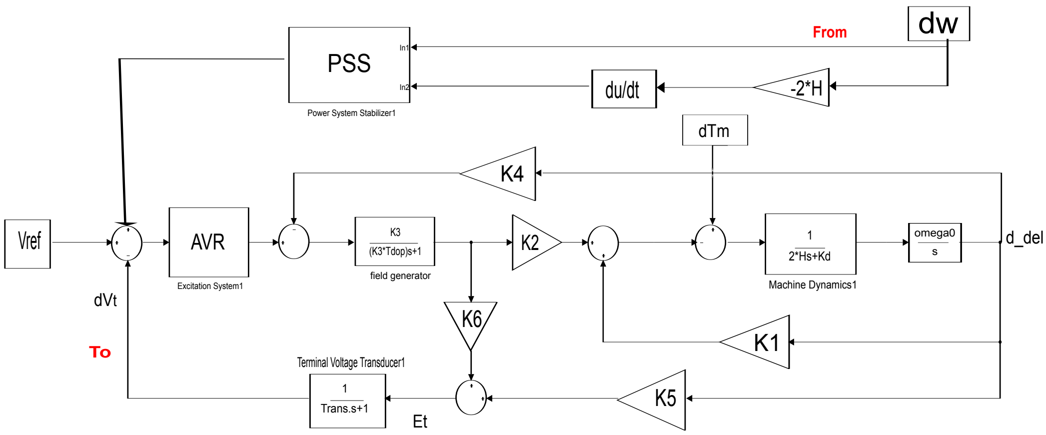

Figure 3.24: SMIB model with PSS requirement1

Table 3.6: operating conditions

	P	Q	Comment
1	Generator off line		No loading
2	0.92569	0.3032	High loading

The operating conditions taken in to account are given in table 3.6. The effective system reactance taken into account is X_e=0.075+j0.713. For a detailed description and derivation of the linearized SMIB system parameters (constants) refer to the appendix.

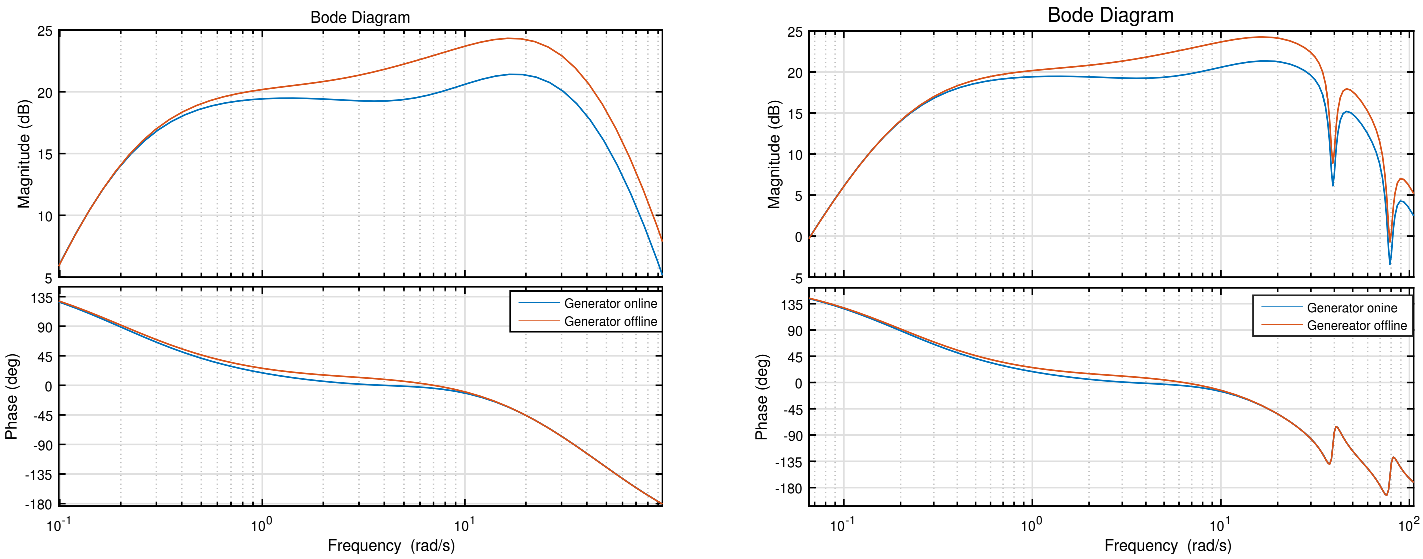

(a) Without notch filter **(b)** With notch filter

Figure 3.25: PSS frequency response taken from speed to terminal voltage for different operating conditions

With reference to the Bode plot given in Figure 3.25, the system phase is remaining within $\pm 90^0$ and close to zero for frequencies in the range of 1-3 Hz. At the same time the gain of the system is around 20dB which can also be increased or decreased depending on the system stability requirement and amount of damping that needs to be added.

3.8.2 PSS stability performance

The PSS should be stable in the control loop of the SMIB in order to maintain the overall stability of the system. This is performed by taking the frequency response with an input from the AVR reference voltage to the output of the PSS while the generator is running at full load as shown in Figure 3.26. As of any linear system stability requirements, the gain should remain less than one while the phase is $\pm 180^o$. The Bode diagram in Figure 3.27 illustrates this requirements are met by the PSS-SMIB forward loop. With the filters the phase margin was found to be 83.8° and gain margin is $16.7dB$ which can also be referred in section 3.7.1.

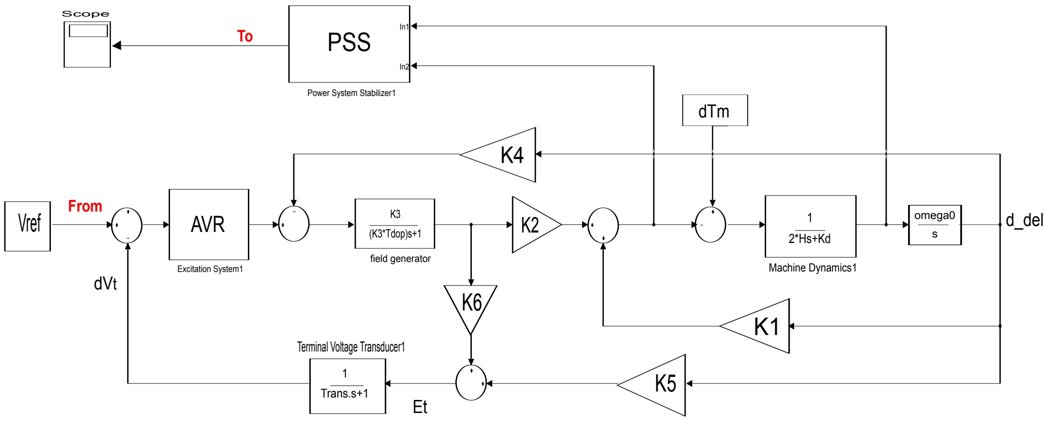

Figure 3.26: Block diagram for signals taken from reference voltage to the PSS output

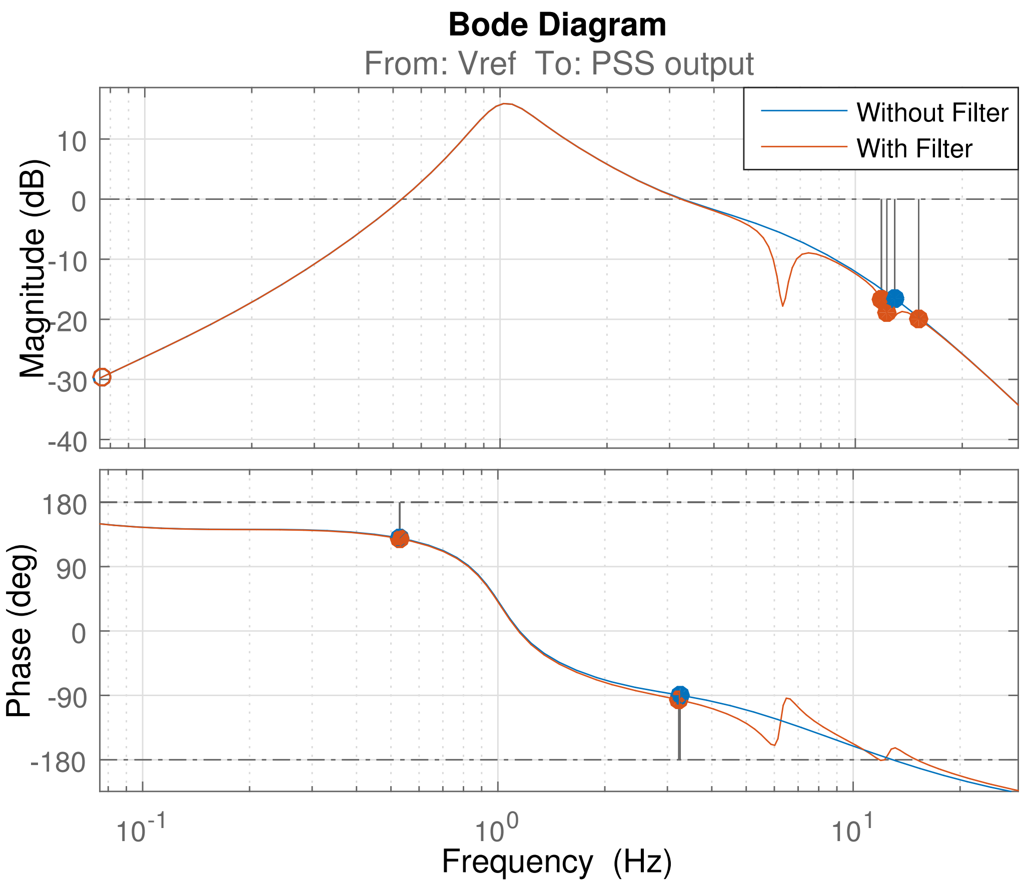

Figure 3.27: Frequency response for requirement 2 after inserting a filter, signals taken from reference voltage to PSS output

3.8.3 PSS noise suppression performance with additional notch filters

The frequency response is taken from mechanical torque to PSS output and is shown in block diagram shown in figure 3.14. It is already explained in Section 3.5.1 the response of the system for different RTF time constants. Here, overall system with all the PSS time constants chosen and the notch filter is shown in Figure 3.28. The requirement for the PSS to suppress the noise is that, it should have a low gain in the frequency range of torque noise. It can be seen from the frequency response that the two notch filters adds to the existing attenuation level at 6.3Hz and 12.55Hz.

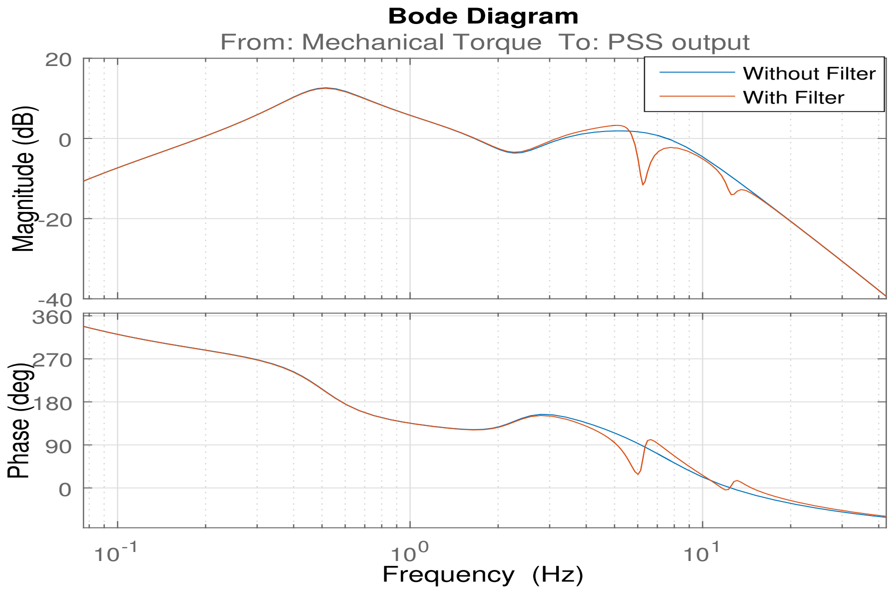

Figure 3.28: SMIB model with PSS (requirement 3) with notch filters for signal taken from mechanical input power to PSS output

4

Matlab Time Domain Simulations and Analysis

The time domain analysis in Matlab is presented in this chapter. First, the simulation is done without any change in mechanical power. Later the synthesised torque noise is injected to the system and the results are presented.

In order to study the action of the PSS, a scenario is simulated with a dip in the reference voltage. The resulting simulations for different parameters are shown in the Figure 4.1 to 4.4. The time domain response shown in Figure 4.1 and 4.2 are for angle and speed respectively. It shows that the PSS helps to improve the damping of oscillations. Figure 4.3 and 4.4, which presents the terminal and field voltage, shows that addition of PSS has an adverse effect.

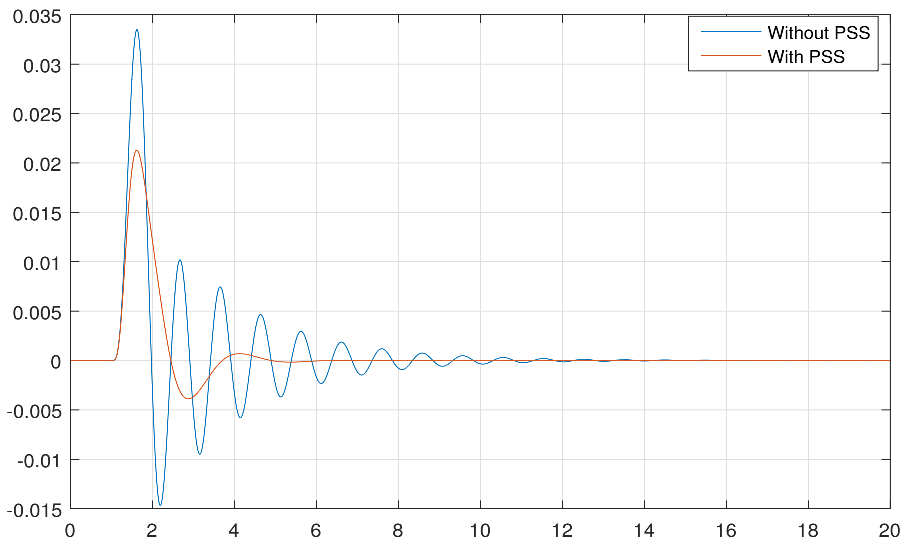

Figure 4.1: SMIB Matlab time domain figures without noise, taken before and after inserting the PSS for angle deviation

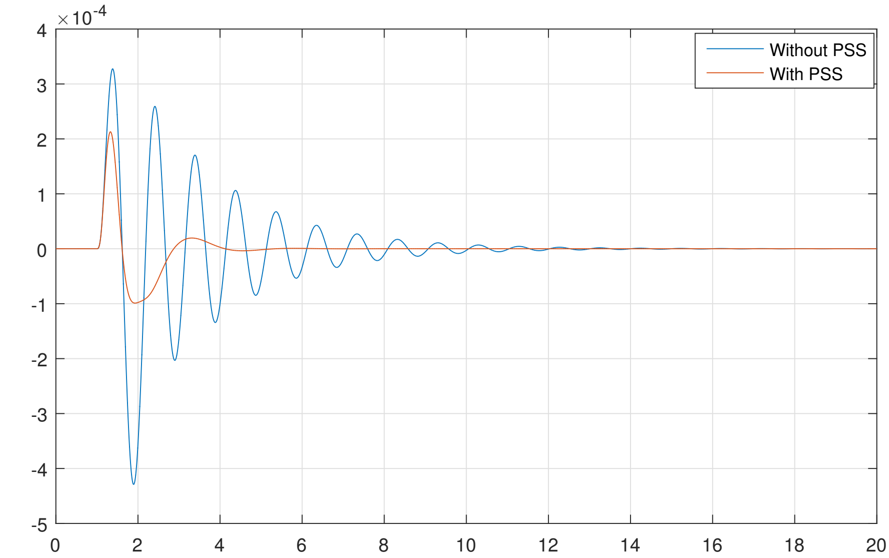

Figure 4.2: SMIB Matlab time domain figures without noise, taken before and after inserting the PSS for Speed deviation

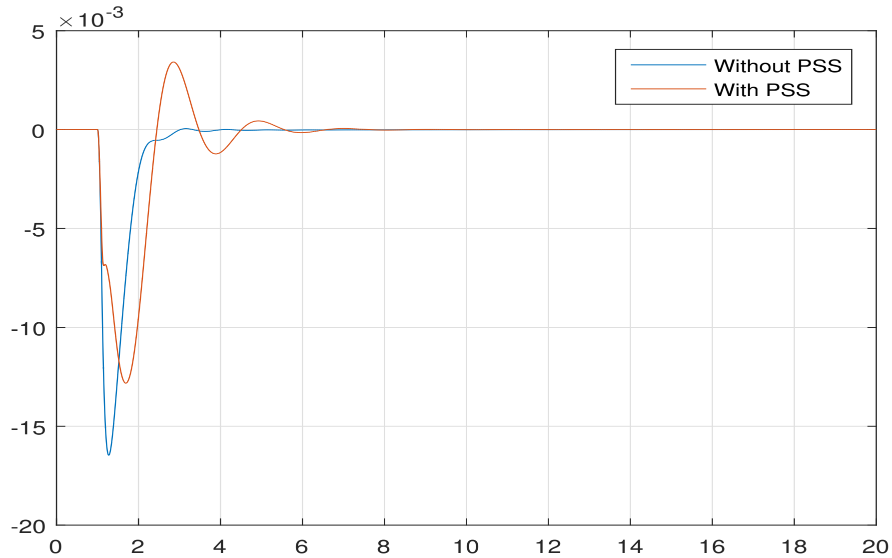

Figure 4.3: SMIB Matlab time domain figures without noise, taken before and after inserting the PSS for terminal voltage

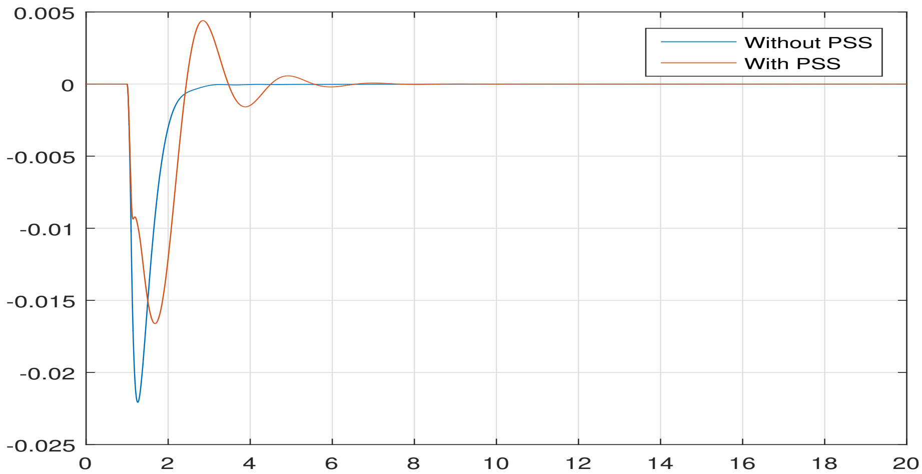

Figure 4.4: SMIB Matlab time domain figures without noise, taken before and after inserting the PSS for field Voltage

The mechanical torque noise that is extracted from the available measurement has been injected to the system to study the output. The torque is derived using the swing equation and is explained in section 3.4. The selected notch filters are also added with the PSS to attenuate the noise.

From the figure given in 4.5, the output of the PSS2B is being greatly reduced after adding the notch filters.

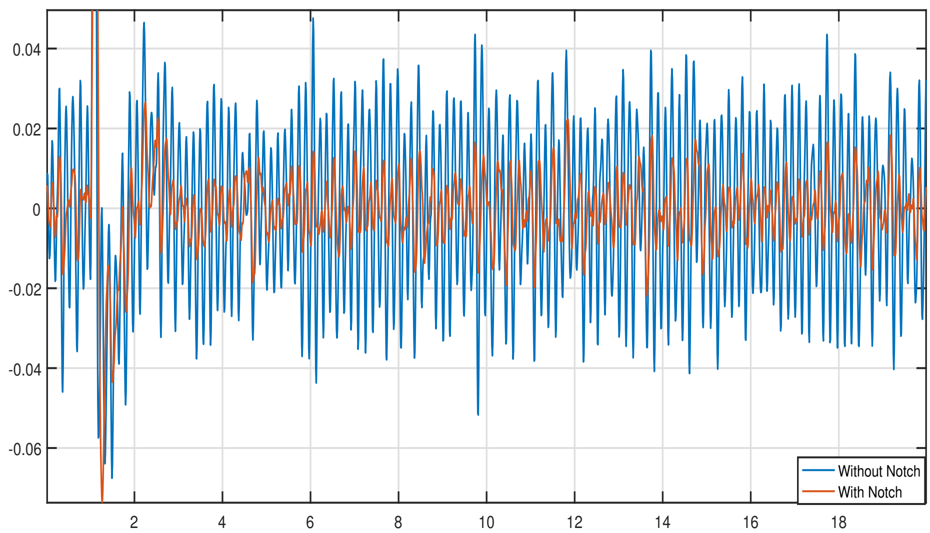

Figure 4.5: PSS2B output signal before and after using the notch filters with mechanical torque noise injected.

The terminal voltage with and without PSS and notch filter is plotted in Figure 4.6 and 4.7. As observed before, the addition of PSS deteriorate the terminal voltage. With the notch filter implemented in the PSS there is a very slight reduction in the noise. The high frequency noise is being removed while the low frequency noise is still present.

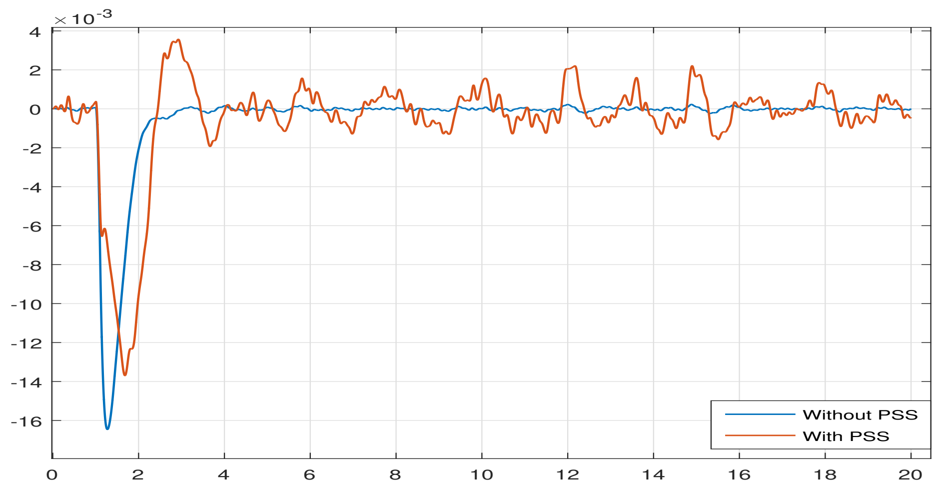

Figure 4.6: SMIB Matlab time domain figure of terminal voltage with synthesised noise with and without PSS.

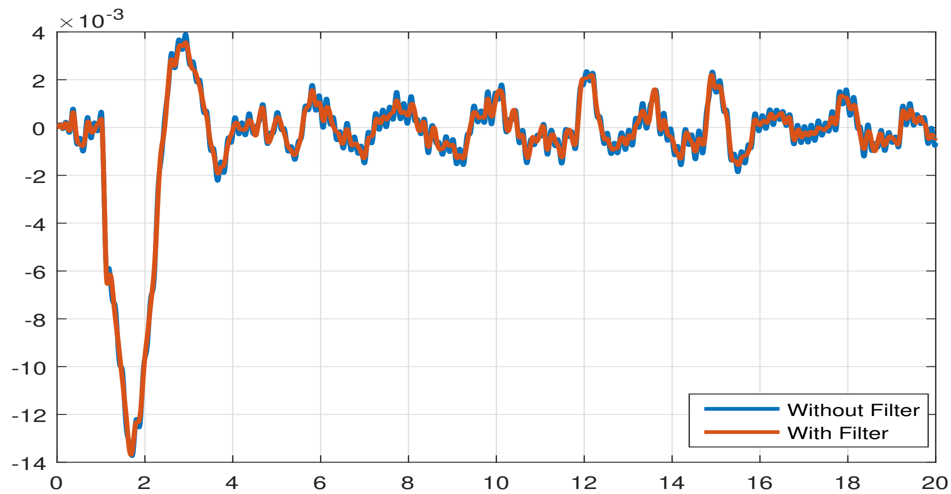

Figure 4.7: SMIB Matlab time domain figure of terminal voltage with synthesised noise with and without notch.

It is also observed that, for speed and angle deviation the addition of PSS improves the damping greatly, but the addition of notch in the PSS does not effect the speed and angle that much.

It can be concluded that the notch filters greatly attenuate the noise in PSS output and has less effect on speed and angle deviation. So notch filter, can be used to reduce the PSS vulnerability to noise there by increasing the PSS performance.

5

PSS performance evaluation using deliberate torque changes

In this chapter, simulations are done to check whether deliberate torque changes can be used to evaluate PSS performance. Several measurement are taken into consideration. The block diagram presented in Figure 5.1 shows signal measurement considered in this investigation. Bode diagrams are plotted for the system with input signals taken from mechanical torque input and reference voltage to:

- PSS2B output
- electrical power
- generator terminal voltage.

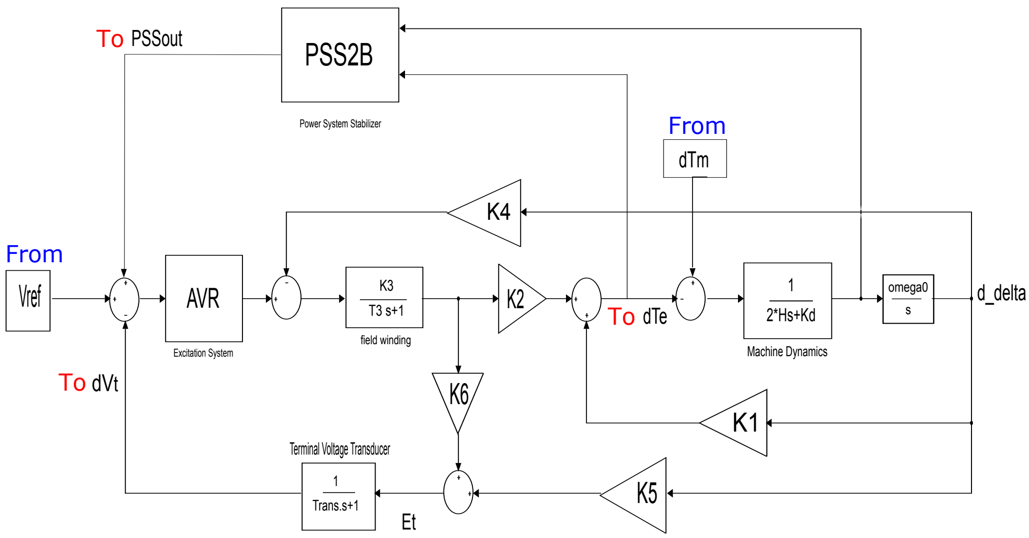

Figure 5.1: SMIB block diagram showing the input and output measurement points

A common method to investigate PSS performance is to take bode plot from voltage reference since it is easily accessible. Here, bode plot is also taken from mechanical torque to further understand the effect of the torque changes on PSS. Bode diagrams are plotted for frequencies in the PSS operating range. This is to examine the changes during PSS off, PSS on that is the normal PSS2B, speed only PSS and power only PSS by changing the RTF cutoff frequency. The last two cases (speed only PSS and power onpy PSS) have been included to evaluate the difference between the input type of the PSS.

5.1 Frequency response of PSS output

The first tested method shows the frequency response taken from mechanical torque or reference voltage to PSS output. In Figure 5.2, the blue line shows when the PSS is turned off. It can be seen that, there is a higher gain around the local mode. This is damped with turning the PSS on as indicated by red line. Since there is a difference between the PSS response when changing the RTF cut-off frequency, it is difficult to distinguish exactly between PSS operation and RTF for the bode plot from mechanical torque. However, regardless of the RTF cut-off frequency, there is a clear gain reduction around the local mode frequency. The same information is obtained from using voltage reference as input (Figure 5.2 (b)). This test is already performed for checking the PSS stability criteria in Section 3.8.2.

It can be concluded that using mechanical torque input gives no additional data than from reference voltage and that this method gives useful information in the local oscillation modes.

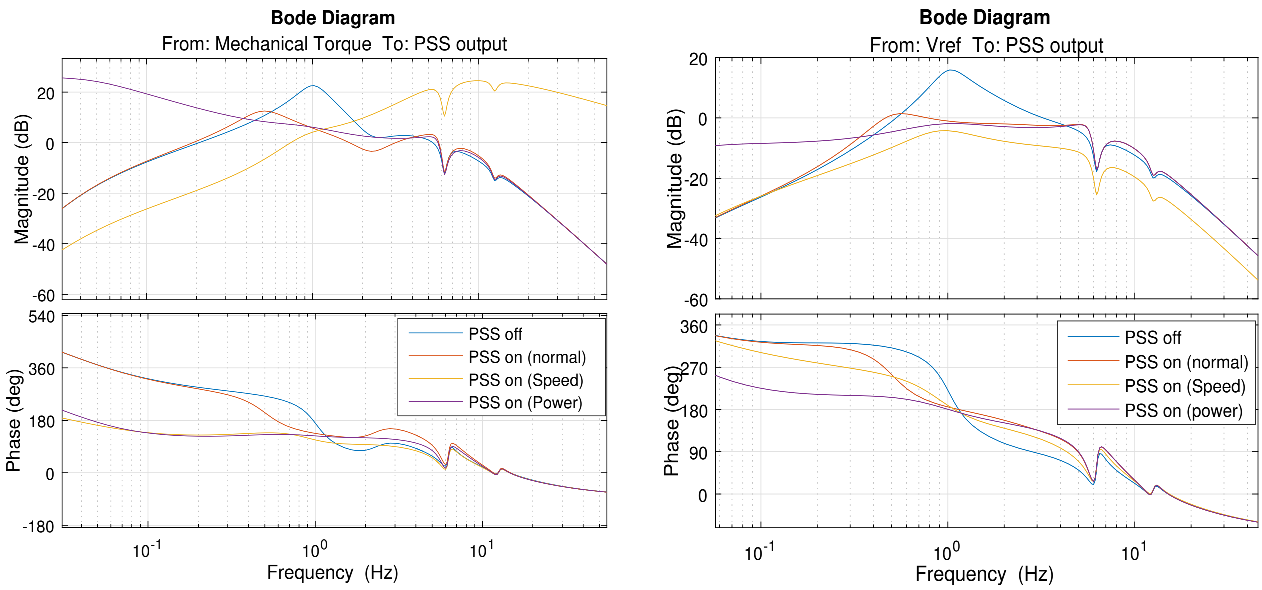

(a) (b)

Figure 5.2: Bode plot to PSS output taken from (a) Mechanical torque (b) Voltage Refrence

5.2 Frequency response of electrical power

The second tested method is the frequency response from mechanical torque or reference voltage to electrical power. The results of both bode plots in Figure 5.3 also give similar information to the previous one on damping performance of the PSS at the local modes around 1 Hz. The figures show the gain of the system reduces with the addition of the PSS. Both bode plot from mechanical torque (a) and voltage reference (b) shows same results.

The conclusion that can be made from this is that there is not much of a difference in using the 1st and 2nd methods for the purpose of studying the PSS damping at local modes. The difference between PSS on and PSS off is smaller in this case than, the first method of using the PSS output.

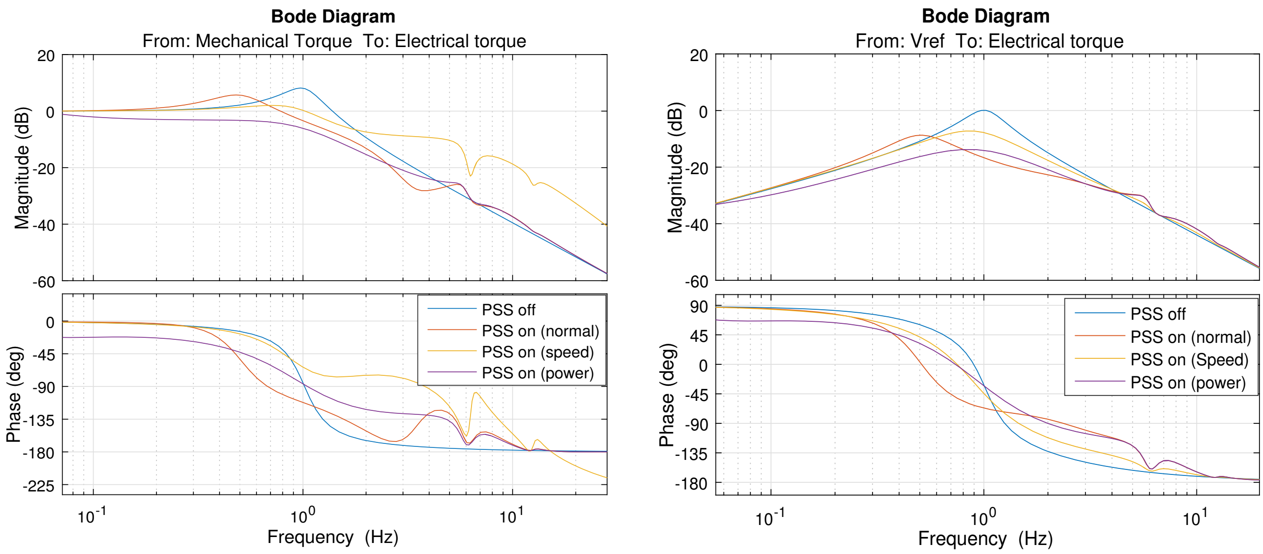

(a) **(b)**

Figure 5.3: Bode plot to Electrical power taken from (a) Mechanical torque (b) Voltage Reference

5.3 Frequency response of terminal voltage

Bode plot presented in Figure 5.4 gives very limited information about the PSS performance. Figure 5.4 (a), from mechanical torque shows that there is an increase in amplitude with the PSS on. This indicates the torque noise sensitivity of the PSS but not its actual damping performance. The figure from reference voltage (b) shows a difference with PSS on and off only in a narrow region at local frequency mode, in a similar manner as for electrical torque as output.

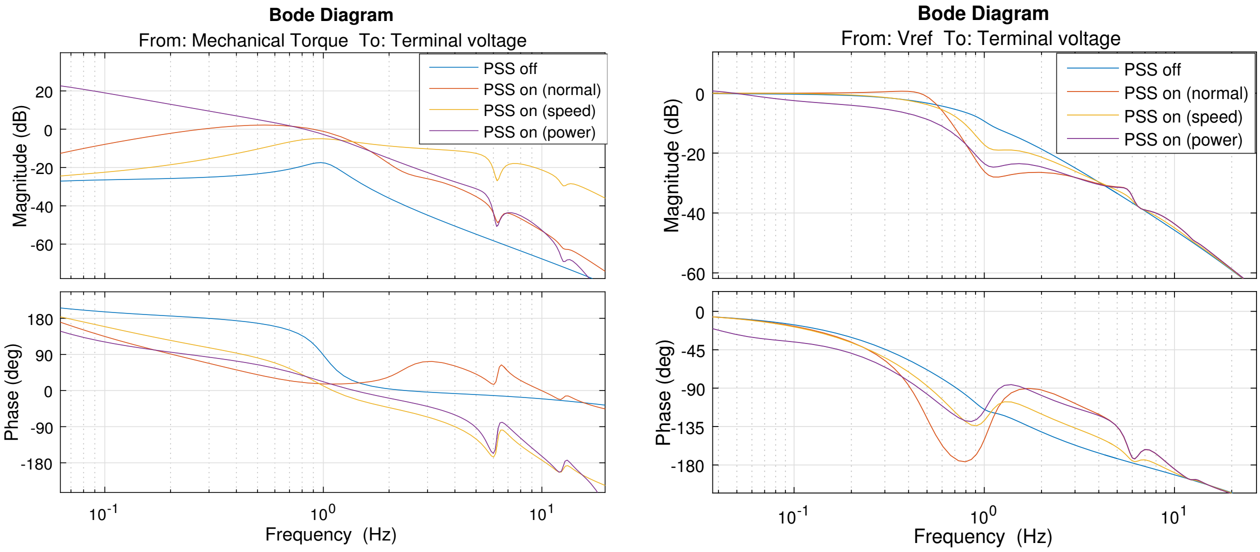

(a) **(b)**

Figure 5.4: Bode plot to Terminal voltage taken from (a) Mechanical torque (b) Voltage Reference

6

Model Verification in Simpow

The SMIB model built in Matlab is verified using power system analysis software Simpow. An AVR model, which is IEEE standard AC7B with a rotating brush-less exciter, is used for simulations. The AVR parameters are set first. Later on, the PSS2B is tuned to damp electromechanical oscillations. Thereafter the notch filters designed to filter the noises created due to torque fluctuations from the reciprocating engine, are included.

6.1 Simpow introduction

Some of the main function of Simpow are:
OPTPOW for the power flow analysis where symmetrical steady state conditions are assumed. The branches are represented by their admittance in positive sequence. The power flow solutions is obtained as the flow of active and reactive power, voltage, current etc.

DYNPOW is used for dynamic calculations. If unsymmetrical networks are analysed, then negative and zero sequence parameters should be given here. The result from Dynpow includes many functions like linear analysis, obtaining time domain plots, eigen value calculation and transient stability.

STAPOW is used for for fault analysis of symmetrical and unsymmetrical states of three-phase power systems. The result of the calculation is currents and voltages in the system at a specified instant of time.

There is a programing language included called Dynamic Simulation Language (DSL). If there is no predefined components, DSL can be used to create it. For example, turbines, governors, machine, PSS, regulators, exciters etc.

6.2 SMIB-Modelling in Simpow

The SMIB model that is built in Matlab, is an ideal model where bus two is being considered as an infinite bus. The ideal design of the system or the assumptions made are compared with a similar model that is built in Simpow. A more realistic model is being considered here so as to show that the parameters from SMIB model can be used in real situations.

The SMIB model built in Simpow is shown in Figure 6.4. The generator used in the model is with one field winding, one damper winding in d-axis and one damper winding in q-axis including the saturation. The generator is connected through a step up transformer and a line of 30KV to the external grid. The generator has a rated power of $27.36MVA$ and other parameters are given in the appendix B. The base values selected is a power of $100MVA$ and frequency of $50Hz$. The other network parameters and their ratings is given below:

Loads- The generator is at the bus 'power plant' where a load, with

- active power $P = 0.5MW$
- and reactive power of $Q = 0.1MVar$ is connected.

Transformer- A step up transformer connected between bus 'power plant' and 'intermediate' has a base power of $30MVA$. Nominal voltage for the primary winding is $30kV$ and secondary winding is $13.2kV$. It also has a short circuit resistance of $0.01p.u.$ and short circuit reactance of $0.0654pu.$.

Line- A line of $20km$ connecting the transformer bus (Intermediate bus) and the external grid has a resistance per km $R = 0.39ohm$ and reactants value of $X =$ 1.09ohms, so there will be some losses in the line.

6.3 AVR Tuning

A detailed AVR tuning procedure is discussed in Section 3.2 using Matlab. In Simpow, a similar procedure is carried out as the AVR tuning is the first step. Effects of generator saturation and demagnetizing effect of the field current is modelled as well.

First, offline operation of the generator is simulated to make sure that the AVR offline performance is within the allowable range. For this a step input in given and the performance of the AVR is analysed. The response after tuning the AVR is shown in the Figure 6.2. The tuned parameters are given in Appendix B (Table B.2).

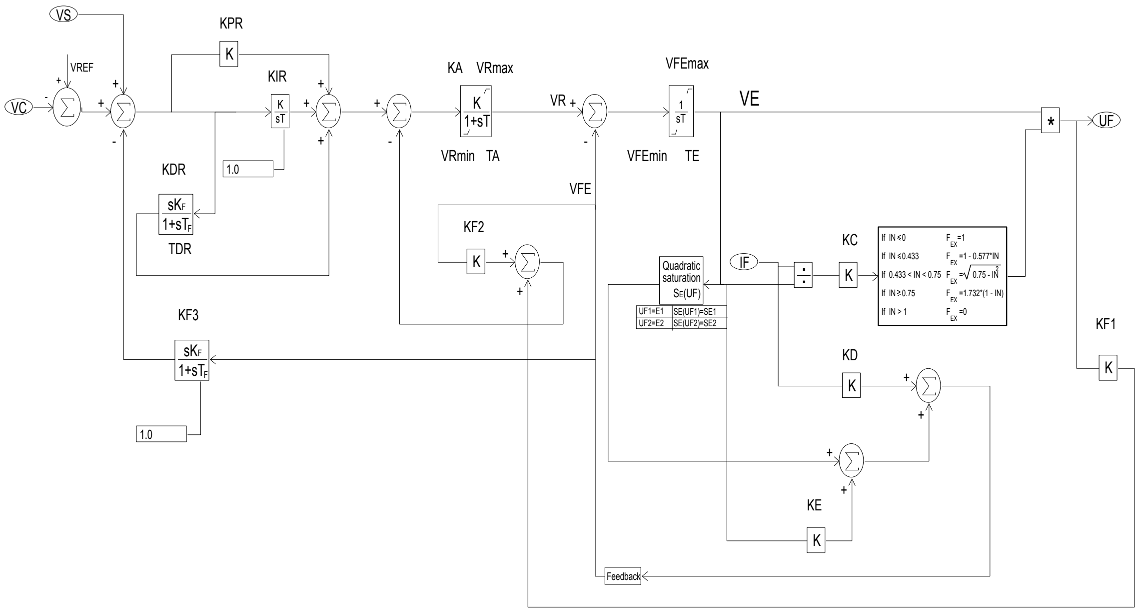

Figure 6.1: AVR AC7B model in HIDRAW

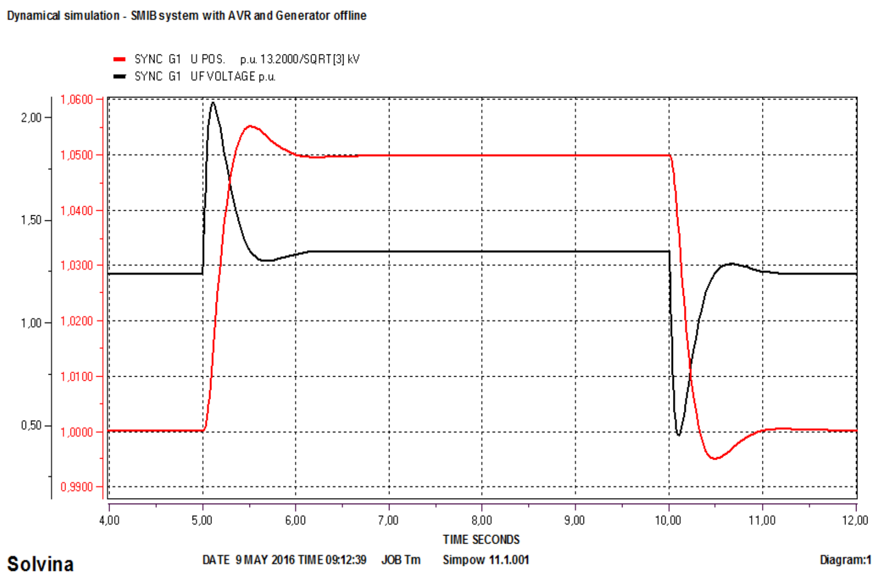

Figure 6.2: Step reponse of an AVR during generator offline operation, with a 5% change in reference voltage in Simpow

The step response with the system kept in offline operation is shown in Figure 6.2. The system is simulated with a 5% change in reference voltage. The rise time of the terminal voltage is within 0.5 seconds for offline operation and settles within 2 seconds which satisfies the AVR tuning condition.

Later, an AVR frequency response is analysed with the system kept at island mode. This is done using a sine wave of known frequency and amplitude as voltage reference input and measuring the generator terminal voltage. The frequency response is plotted in Figure 6.3. The result shows that the AVR response in PSS operating range is as expected as in chapter 3.2, that is the terminal voltage phase lag increases with increase in frequency. It can be compared with Matlab in Figure 2.8.

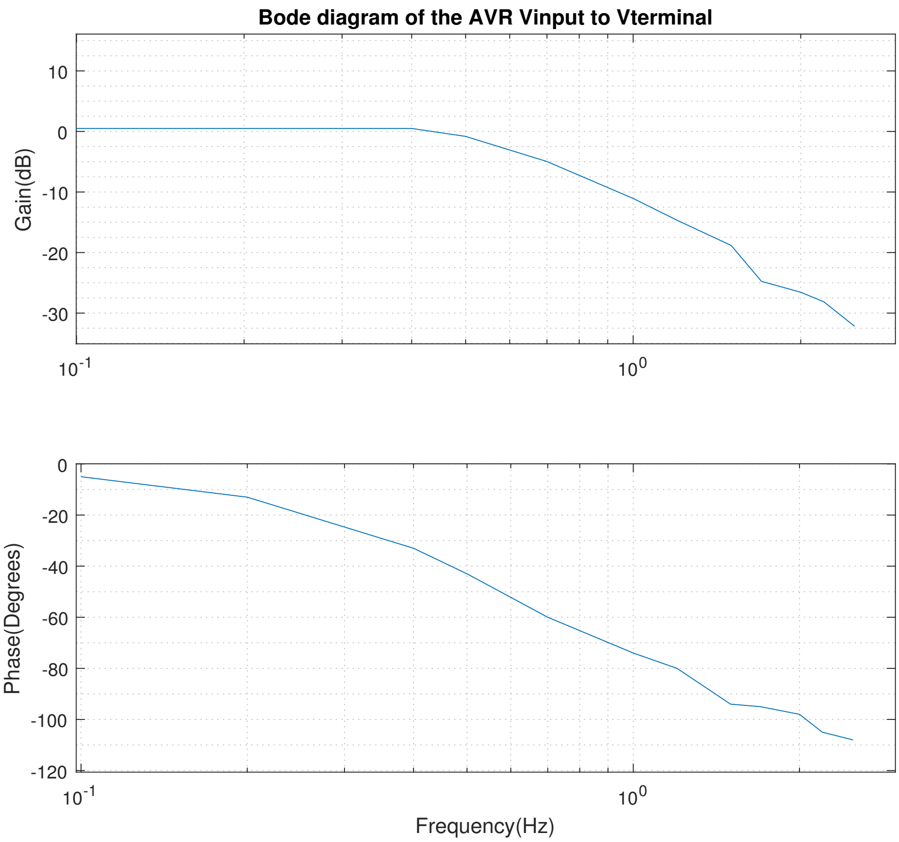

Figure 6.3: AVR frequency response during generator offline(island mode), signal taken from AVR input to the terminal voltage

6.3.1 System on-line performance

After tuning the AVR in offline operation, the system is reconnected to the external grid. The power result is shown in Figure 6.4. As can be seen, for the power generation of 21 MW there is an angle deviation of 28.8° at generator bus. The system is at steady state with the infinite grid compensating for the production.

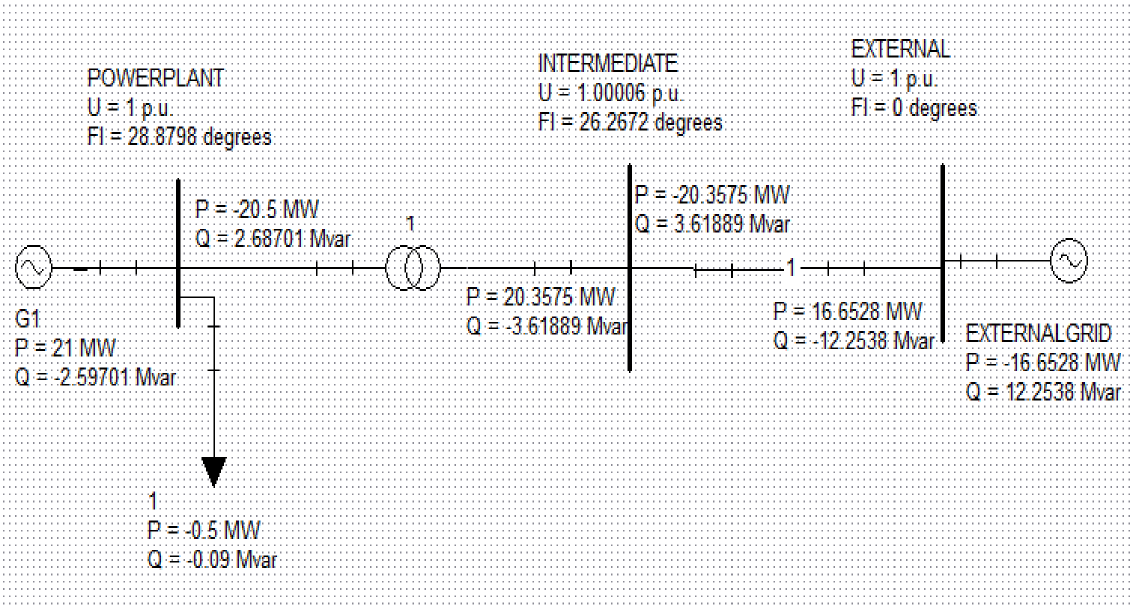

Figure 6.4: Single line diagram of SMIB model in simpow

A transmission line fault is created at 1 second and is cleared at 1.05 seconds. The performance of the generator for bringing the bus voltage and frequency to nominal level, is examined. In addition, the level of damping for oscillations of different modes is studied.
After studying the oscillatory modes of the system, the PSS2B is being tuned to add more damping. The results of the simulation result for various network parameters are plotted in Figures 6.5 and 6.6.

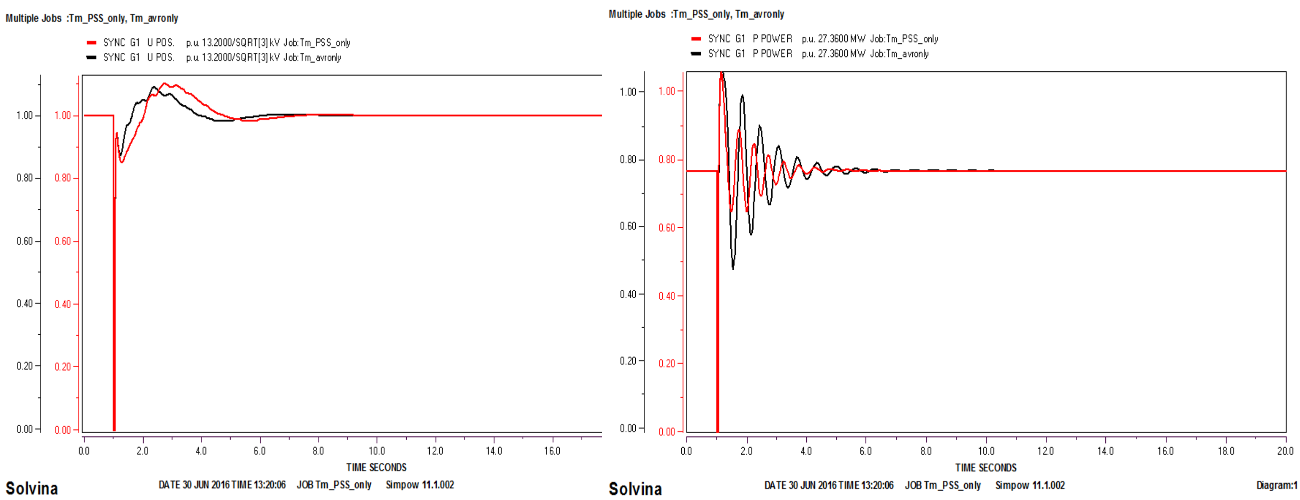

(a) Terminal voltage **(b)** Generator power

Figure 6.5: Simpow time domain plot before adding PSS in black color and after adding the PSS in red color.

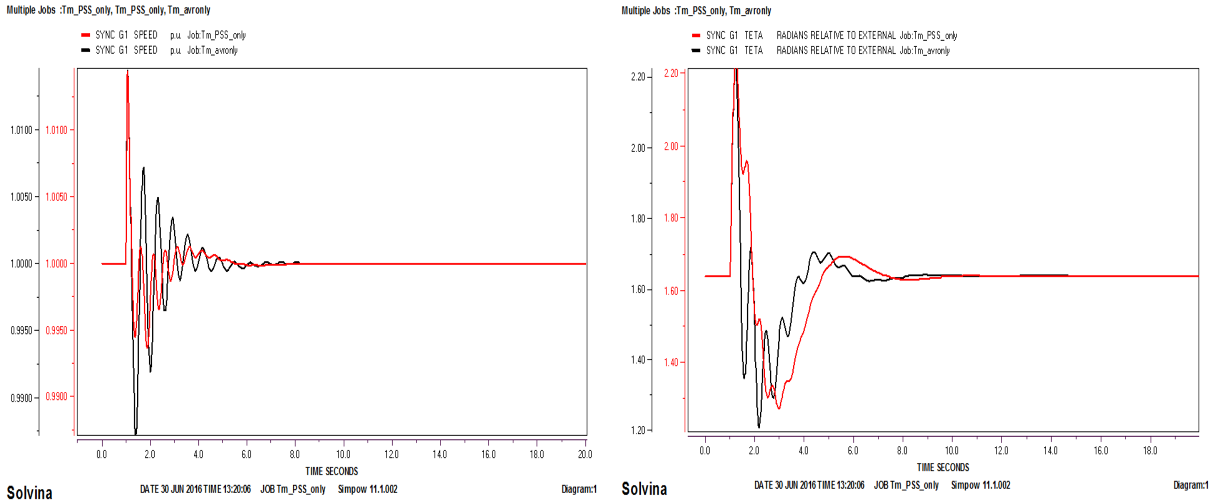

(a) Rotor speed **(b)** Rotor angle

Figure 6.6: Simpow time domain plot showing speed and angle, before adding PSS in black and after adding the PSS in red

The results show the performance of the AVR and PSS for electromechanical oscillation damping as well as restoring the stable operation of the system after a fault condition. Prior to the fault point from 0 to 1 seconds, the system is working at steady state. At 1 second, a fault is introduced at the transmission line connecting the generator bus with the grid (synthetic infinite bus). The generator power and bus voltage drops to a low value nearly zero. The AVR tries to bring the terminal voltage to a normal value by increasing the field voltage. The system oscillates due to inertia, and finally manages to come to stable operation after around 10 second instant.
After adding the PSS2B, it is clear that the oscillations are damped to a considerable amount thus reducing the settling time. This is denoted by the red lines in Figures 6.5 and 6.6.

6.4 PSS2B torque noise reduction in Simpow

The tuned PSS2B is being verified in order check its capability to suppress fluctuation of the reciprocating torque. For studying the frequency domain the system is simulated using a sine wave with selected frequencies at the mechanical torque input of the synchronous machine. The frequency response of the system from mechanical torque input to the PSS2B output is being studied. The results of the simulation done are given in Figure 6.7.

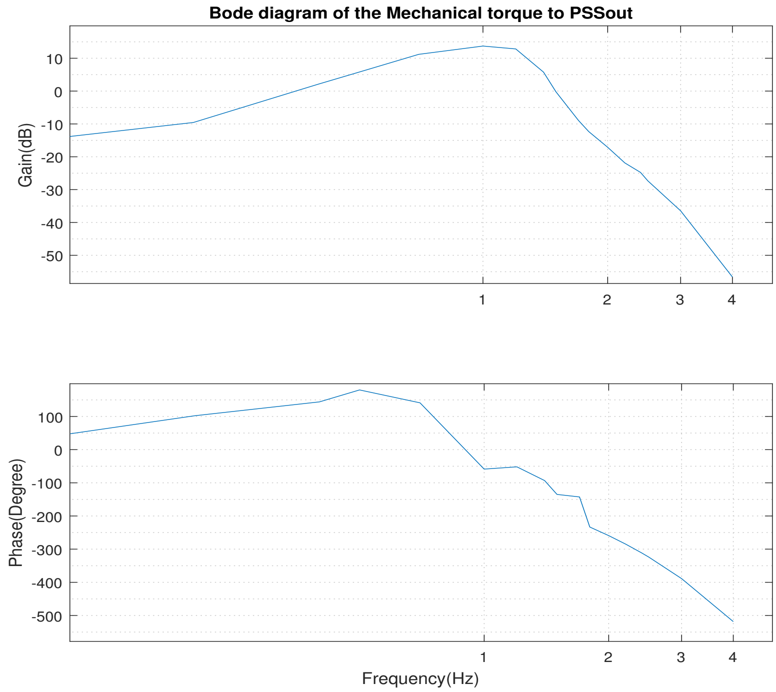

Figure 6.7: Frequency response taken from Mechanical torque to PSS2B output for a range of frequency from 0.1 to 4Hz for noise reduction performance verfication test

For bode plot shown in Figure 6.7, it can be noted that the PSS2B gain response decays on the two sidebands of frequencies outside the PSS2B operating region. The steep roll-off in gain at frequencies above 2Hz proves the PSS2B is capable of reducing torque noises above these frequencies. In addition to this, notch filters can be incorporated within the PSS2B to improve the gain response at particular frequencies. This result verifies to the one which was simulated in Matlab using the linearized SMIB model bode diagram in Figure 3.28.

The real time torque noise that was extracted using Matlab, is used here for studying the time domain response. The noise signal is being added to the mechanical input of the system. A similar PSS2B as in Matlab is used here. The values of PSS2B parameter that was used in Matlab, given in Appendix B, is also used here with the difference being that 3^{rd} lead lag is not used, that is time constant is made equal $T10 = 0.1, T11 = 0.1$. Some of the generator parameters with and without PSS2B is shown in Figures 6.8 and 6.9.

Figure 6.9 and 6.8 shows the angle and speed deviation with the real noise injected to the system. The PSS2B has improved the initial oscillations of the system effectively. In case of angle deviation the initial transients are damped but an overshoot is observed.

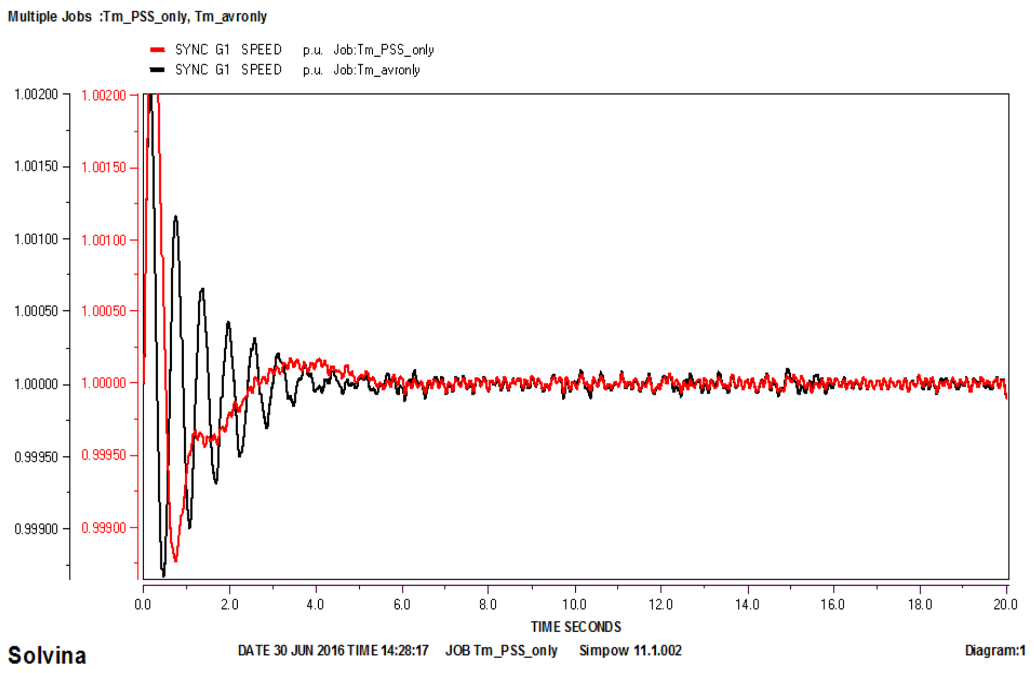

Figure 6.8: Simpow time domain plot with noise injected showing speed without PSS by black lines and with PSS by red lines

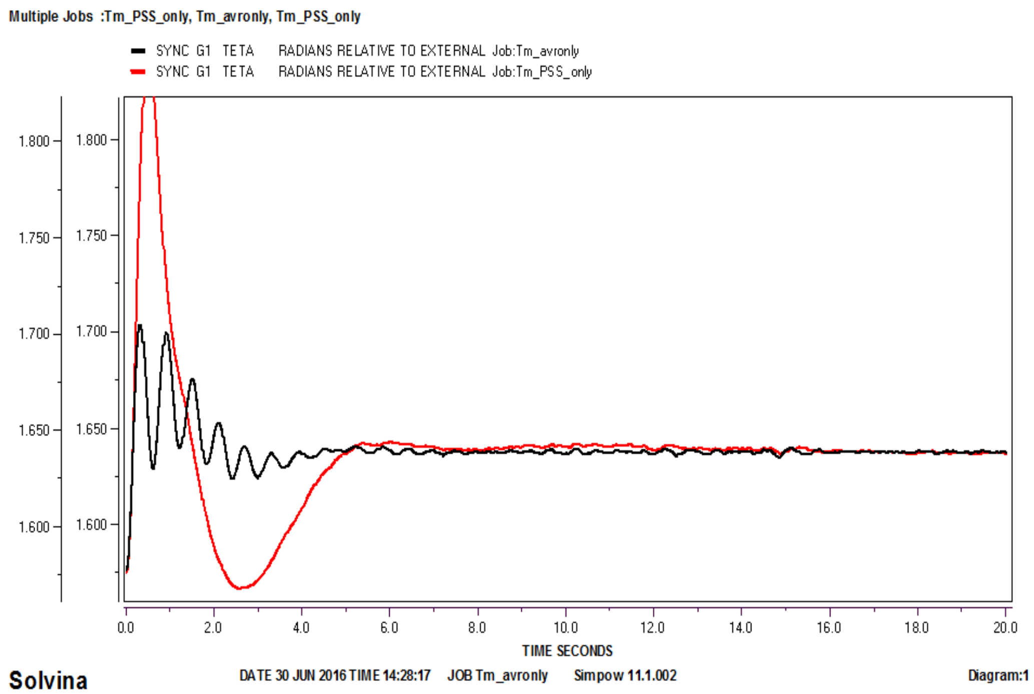

Figure 6.9: Simpow time domain plot with noise injected showing angle without PSS by black lines and with PSS by red lines

The Figure 6.10 shows the variation of PSS2B output with the addition of a notch filter. The initial transients is not shown here. The figure is zoomed from 6 seconds to 20 seconds so as to clearly see the difference with the addition of notch. All the other figures or simulations shown in this chapter are from 0 seconds to 20 seconds showing the initial transients. The result is similar to the one obtained in Matlab. As can be seen with the addition of the notch the PSS2B output is reduced to a good extent.

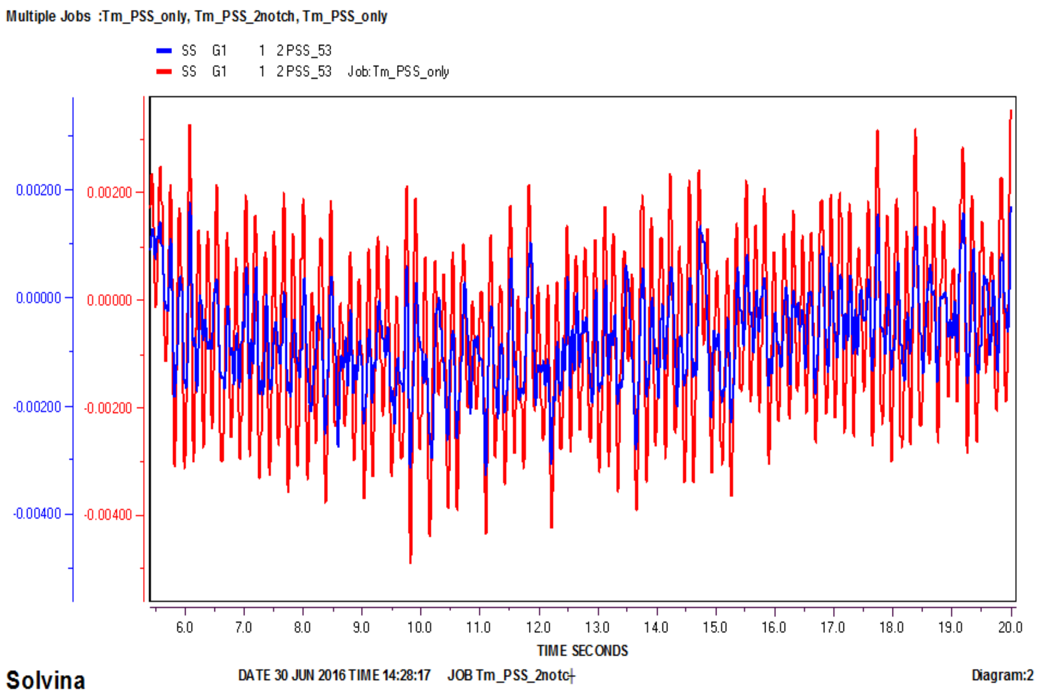

Figure 6.10: PSS2B output, with PSS before inserting notch is indicated by red lines and with PSS+notch filters indicated by blue line

The Figure 6.11 shows the various generator parameters such as terminal voltage, field voltage, genrator active and reactive power with PSS2B and notch filters implemented.

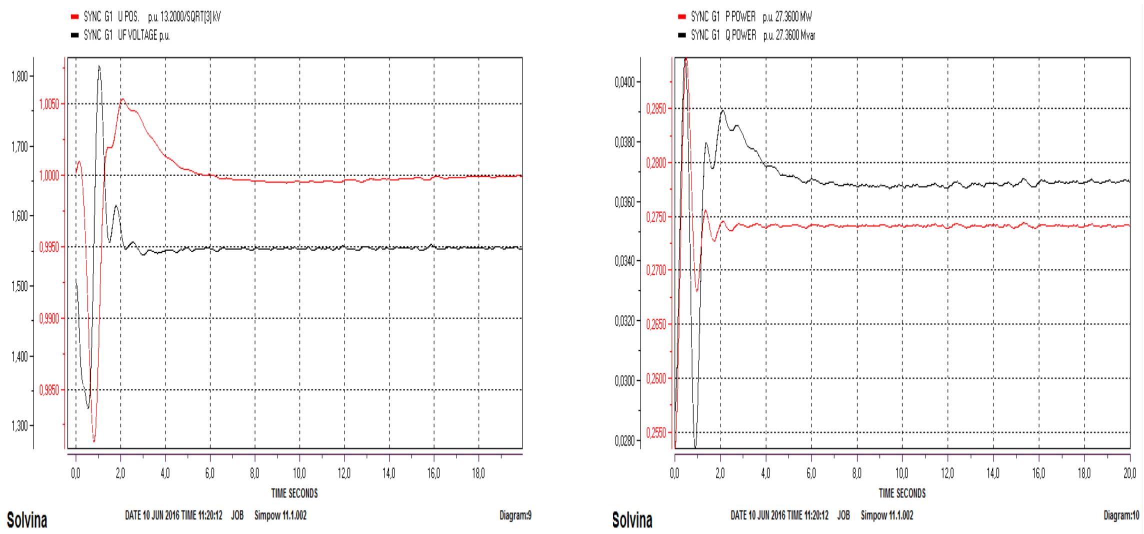

(a) Vf and Vt **(b)** Gen. P and Q

Figure 6.11: Simpow time domain plot showing (a) terminal voltage in red line and field voltage in black line (b) real power in red line and reactive power in black line

The conclusion that can be drawn from the verification of results in Simpow is that a similar results as in Matlab is achieved. PSS2B and the chosen notch filter has effectively reduced the influence of torque noise.

7

Conclusions and Future works

7.1 Conclusions

PSS2B design is evaluated for reciprocating engines using a linearised SMIB model for frequency domain and time domain analysis. A case study is also performed using a real time measurement data containing torque noise. In addition, the use of filters, specifically notch filters, are investigated for attenuation of noise originating from the reciprocating engine torque. Finally, it is studied how a deliberate engine torque changes can be used to evaluate the PSS performance.

The evaluation revealed that the choice of different time constants of the RTF affects the system's vulnerability to fluctuations in the engine torque. Therefore, a proper RTF time constants are chosen so that there is more damping so the overall system performance is improved. It is found that the size of filters added to mitigate torque noise has an effect on the stability margins of a system. Hence, proper choice of filter sizes is very important to ensure the systems stable operation. Consequently, appropriate dimensioning of notch filters needs to be done to attenuate the noise from the engine without degrading the general stability of the system. It can also be concluded that deliberate mechanical input variations will reveal the PSS performance at local oscillations modes only.

The simulations performed in Simpow with the SMIB network shows similar results tom Matlab simulations. The system stability is found to be enhanced with the use of the above mentioned methods and the torque noise is attenuated greatly. The time domain simulations performed for various signals using the SMIB model in Matlab and Simpow show that the system has good damping.

7.2 Future Works

Even though the current methods works well and the overall system performance is satisfactory, for further enhancement more investigations could be conducted. Some of the possible future work of this thesis are:

- A further performance evaluation could be performed for multi-machine infinite bus model to get more information on the effectiveness of the PSS2B with regard to reciprocating engine torque noise .
- A more complex structure of the multi-band PSS4B can be used for filtering out the torque noise.
- Band reject filters can be investigated for noise attenuation in a wider range of frequencies.

Bibliography

[1] P. Kundur, "Power System Stability and Control", Mcgraw Hill Inc., Palo Alto, California, USA, 1994.

[2] E. Ciapessoni, D. Cirio, A. Gatti, A. Pitto, Renewable Power integration in sicily: frequency stability issues and possible countermeasures, IEEE 2013.

[3] M.J.Gibbard, P.Pourbeik, D. J. Vowles, "Small-signal stability control and dynamic performance of power systems", University of Adelaide Press, Adelaide, 2015.

[4] O.Samuelsson, Power system damping: Structural aspects of controlling active power, Lund Institute of Technology, Lund, Sweden, 1997.

[5] G. Rogers, "POWER SYSTEM OSCILLATIONS", 1st Edition, Springer Science+Business Media, LLC, New York, USA, 2000.

[6] H. Saadat, "Power System Analysis", PSA Publishing Inc, Milwaukee, USA, 2010.

[7] IEEE-Standard-421.5, IEEE Standard Definitions for Excitation Systems for Synchronous Machines,, December 2005.

[8] P.P.deMello, C.Concordia, Concepts ofSysnchronous machine Stability As Affected by Ecxitation control, General Electric Company, Schenectady, New York, 1952.

[9] K. R. Padiyar, "POWER SYSTEM DYNAMICS Stability and control", second edition Edition, BS Publications., Hyderabad, USA, 2008.

[10] F.P.DeMello, T.L.Laskoswski, Concepts of power system dynamic stability, Vol. PAS 94, May/June 1975.

[11] S.B.Crary, Power System Stability, John Wiley and Sons Inc., 1955.

[12] w. E. L. A. D. J. O. Graham J.Dungeon, J. R. McDonald, The Effective role of the AVR and PSS in power systems: Frequency Response Analysis, IEEE, November 2007.

[13] E.V.Larsen, D.A.Swann, "Damping for the Northwest-Southwest Tie Line Oscillations-An Analog Study,", Vol. Vol. PAS-85, IEEE Transactions on Power Apparatus and Systems, IEEE Trans,, December 1966.

[14] J. W. J. Machowski, J.R.Bumby, "Power system dynamics: stability and control.", Wiley, Chichester, 2008.

[15] G. R. Bérubé, L. M. Hajagos, "Accelerating-Power Based Power System Stabilizers", Mississauga, Ontario, Canada.

[16] R. L. Dr. A. Murdoch, S. Venkataraman, W. Pearson, Integral of accelerating power type pss part 1 - theory, design, and tuning methodology, IEEE Transactions on Energy Conversion (Volume:14 , Issue: 4).

[17] E. Larson, D. Swann, Applying power system stabilizers, part iii practical considerations, IEEE transaction on power apparatus and systems Vol. PAS-100 (6 June 1981) 3034–3046.

[18] S. Yee, Coordinated tuning of power system damping controllers for robust stabilization of the system, Ph.D Thesis,University of Manchester,Faculty of Engineering and Physical Sciences,Manchester, England.

[19] A.Heniche, I.Kamwa, R.Grondin, "Torsional-mode identification for turbo generators with application to PSS tuning", Springer., Montreal Canada, June 2005.

[20] W.G.Heffron, R.A.Phillips, Effect of a Modern Amplidyne Voltage Regulator on Underexcited Operation of Large Turbine Generators, IEEE (August 1952) 692–697.

Appendices

A

Appendix A

Linearized SMIB parameters

The linearized SMIB model parameters and their mathematical equation is given as follows. First let us consider the Single machine infinite bus single line diagram given below.

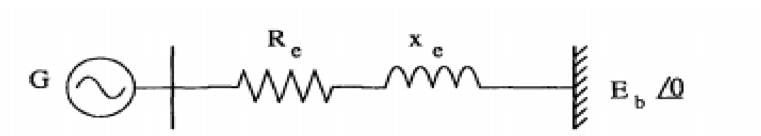

Figure A.1: Single line diagram of a typical power system

Key:
The single line diagram and SIMB model.

Annotation given in the steady state mathematical expression are:
Parameters Values can be given either in per-unit or in actual values E_B= System base voltage in
E_t= Generator terminal voltage
$E^{'}$= Generator internal voltage (Induced voltage)
R_e =Line resistance
δ_0= initial rotor angle
X_E = Transmission line reactance
δ = Rotor angle
$X_d^{'}$ = Transient Machine reactance
$X_d^{''}$ = Sub-transient reactance
X_T = Total reactance
K_s = Synchronizing torque coefficient
K_d = Damping torque coefficient
ω_r = Rotor speed

p = differential operator
H = Machine inertia constant
$T_{d0}^{'}$ =d-axis transient open circuit time constant
$T_{q0}^{'}$= q-axis transient open circuit time constant
$T_{d0}^{''}$= d-axis sub-transient open circuit time constant
$T_{q0}^{''}$= q-axis sub-transient open circuit time constant
T_{d0}= d-axis steady state open circuit time constant
i_d = d-axis stator current
i_q = q-axis stator current
X_d= d-axis stator reactance
X_q= q-axis stator reactance
e_{d0} = d- axis voltage component
e_{q0} = q-axis voltage component
$\psi_f d$ = air gap flux linkage
T_e = Electrical torque

Field Circuit Dynamics

The field circuit equation in the dq reference frame can be represented as equation A.1 [1].

$$p\psi_f d = \omega_o(e_{fd} - R_{fd} i_{fd}) \tag{A.1}$$

Where:
$p\psi_{fd}$=change in air gap flux between the rotor and the stator
R_{fd} = field winding resistance
e_{fd} = d-axis field voltage
Equations 2.4,2.5 and A.1 describe the machines dynamics of including the effect of the field winding $\Delta\psi_{fd}$. In order to represent the variables in equation A.1 $\Delta\psi_{fd}$ as a function of the state variables, ΔT_e and i_{fd} has were modified. From the basic electromagnetic equations, small perturbations in field current and air gap torque can be used for as follows [9]:

$$\Delta I_{fd} = \frac{\Delta\psi_{fd}}{L_{fd}} \tag{A.2}$$

$$\Delta T_e = \psi_{ad}\Delta i_q - \psi_{aq}\Delta i_d \tag{A.3}$$

Here $\Delta\psi_{fd} = \Delta\psi_{aa} - \Delta\psi_{aq}$ is the change in mutual air gap flux linkage. Similarly the electrical from the network circuit equation d axis and q axis voltage relationships has the following format[Padiyar K.R].

$$e_q = R_e i_q - X_e i_q + E_b cos(\delta) \tag{A.4}$$

$$e_d = R_e i_d - X_e i_d - E_b sin(\delta) \tag{A.5}$$

Expressing the network equations A.5 in terms of i_d and i_q and linearising gives an equation below [9]:

$$\Delta i_d = m_1 \Delta\delta + m_2 \Delta\psi_{fd} \tag{A.6}$$

$$\Delta i_d = n_1 \Delta\delta + n_2 \Delta\psi_{fd} \tag{A.7}$$

Where:
$m_1 = \frac{1}{z}(R_e.E_b cos(\delta) - (X_q + X_e)E_b sin(\delta_o)$
$m_2 = \frac{1}{z}(-X_q - X_e)$
$n_1 = \frac{1}{z}((X'_d + X_e)E_b cos(\delta_o) + (R_e E_b sin(\delta_o))$
$n_2 = \frac{R_e}{Z}$
and $Z = (X'_q + X_e)(X_q + X_e) + R_e^2$

Hence after representing the flux linkage as a function of the state variables the linearized state space model of the synchronous machine sdynamcis including the effect of the field winding can written as equation A.8 below [1]

$$\begin{bmatrix} \dot{\Delta\omega_r} \\ \dot{\Delta\delta} \\ \dot{\Delta\psi_{fd}} \end{bmatrix} = \begin{bmatrix} b_{11} & b_{12} & b_{13} \\ \omega_o & 0 & 0 \\ 0 & b_{32} & b_{33} \end{bmatrix} \begin{bmatrix} \Delta\omega \\ \Delta\delta \\ \Delta\psi_{fd} \end{bmatrix} + \begin{bmatrix} c_{11} & 0 \\ 0 & 0 \\ 0 & c_{32} \end{bmatrix} \begin{bmatrix} \Delta T_m \\ \Delta E_{fd} \end{bmatrix} \tag{A.8}$$

Similarly this equation also introduces constants K_1,K_2,K_3 and K_4 that represent the effect of change in rotor angle and field voltage on the damping and synchronizing components of the electromagnetic torque or electrical torque and are called Heffron Phillips constants [20]. They are given by the relationships given in equations A.9 to A.12. These parameters are dependent on system parameters and could change their values with the operating conditions of the synchronous machine [20] and their relationship with the network parameters and operating conditions of the machines are given below: [9].

Where:
$b_{11} = \frac{-K_D}{2H}$ $\quad b_{12} = \frac{-K_1}{2H}$
$b_{13} = \frac{-K_2}{2H}$ $\quad b_{21} = \omega_o$
$b_{33} = \frac{-\omega_o R_{fd}}{L_{fd}} + m_1.L'_{ads}$
$c_{11} = \frac{1}{2H}$ $\quad c_{32} = \frac{\omega_o.R_{fd}}{L_{adu}}$

$$K_1 = E_{qo} n_1 - (X_q - X'_d) i_{qo} m_1 \tag{A.9}$$

$$K_2 = E_{qo} n_2 + i_{qo} - (X_q - X'_d) i_{qo} m_2 \tag{A.10}$$

$$K_3 = \frac{1}{(1 - (X_d - x'_d) m_2)} \tag{A.11}$$

$$K_4 = -(X_d - Xd') m_1 \tag{A.12}$$

$$K_5 = \frac{e_{d0}}{E_{t0}}[-R_a m_1 + L_l n_1 + L_{aqs} n_1] + \frac{e_{q0}}{E_{t0}}[-R_a n_1 + L_l m_1 + L'_{ads} m_1] \tag{A.13}$$

$$K_6 = \frac{e_{d0}}{E_{t0}}[-R_a m_2 + L_l n_2 + L_{aqs} n_2] + \frac{e_{q0}}{E_{t0}}[-R_a n_2 + L_l m_2 + L'_{ads}(\frac{1}{L_{fd}} - m_2)] \quad \text{(A.14)}$$

In a simplified format the constants K_5 and K_6 that are being used to calculate the parameters can be written as below.

$K_5 = -(\frac{e_{do}}{E_{to}})X_q n_1 + (\frac{e_{qo}}{E_{to}})X'_d m_1$

$K_6 = -(\frac{e_{do}}{E_{to}})X_q n_2 + (\frac{e_{qo}}{E_{to}})(1 + X'_d m_1)$

The state space representation of the model in Figure 2.6 becomes

$$\begin{bmatrix} \Delta\dot{\omega}_r \\ \Delta\dot{\delta} \\ \Delta\dot{\psi}_{fd} \\ \Delta\dot{v}_1 \end{bmatrix} = \begin{bmatrix} b_{11} & b_{12} & b_{13} & 0 \\ b_{21} & 0 & 0 & 0 \\ 0 & b_{32} & b_{33} & b_{34} \\ 0 & b_{42} & b_{43} & b_{44} \end{bmatrix} \begin{bmatrix} \Delta\omega \\ \Delta\delta \\ \Delta\psi_{fd} \\ \Delta v_1 \end{bmatrix} + \begin{bmatrix} e_{11} \\ 0 \\ 0 \\ 0 \end{bmatrix} \begin{bmatrix} \Delta T_m \end{bmatrix} \quad \text{(A.15)}$$

B

Appendix B

Synchronous Generator Parameters

Table B.1: Generator parameters

Parameter Description	Value	Unit
Rated apparent power, S_n	9.12	MVA
Rated voltage, V_n	13.2	kV
Rated frequency, f_n	50	Hz
Total inertia constant, H	1.36	s
Rated power factor, PF	0.8	-
d-axis synchronous reactance, X_d	2.764	p.u.
d-axis transient reactance, X'_d	0.329	p.u.
d-axis subtransient reactance, X''_d	0.233	p.u.
q-axis synchronous reactance, X_q	2.703	p.u.
q-axis transient reactance, X'_q	0.760	p.u.
q-axis subtransient reactance, X''_q	0.305	p.u.
Stator leakage reactance, X_l	0.143	p.u.
d-axis short circuit transient time constant, T'_d	0.38	s
d-axis short circuit subtransient time constant, T''_d	0.03	s
q-axis short circuit transient time constant, T'_q	0.12	s
q-axis short circuit subtransient time constant, T''_q	0.03	s
Field resistance, R_f	0.229	Ohm
Field resistance reference temperature, T_{ref}	20	°C

The values of parameter for the diesel engine driven power plant generator used for modelling are given in the table B.1.

Excitation system Parameters

The values of parameters for IEEE AC7B is given in the table B.2

Table B.2: Brushless excitation system parameters

Parameter Description	Value	Unit
Voltage regulator proportional gain, K_{PR}	20	p.u.
Voltage regulator integral gain, K_{IR}	25	p.u.
Voltage regulator derivative gain, K_{DR}	5	p.u.
Lag time constant, T_{DR}	0.003	s
Voltage regulator proportional gain, K_{PA}	1	p.u.
Voltage regulator integral gain, K_{IA}	0.01	p.u.
Excitation control system stabilizer gain, K_{F1}	0	p.u.
Excitation control system stabilizer gain, K_{F2}	0	p.u.
Excitation control system stabilizer gain, K_{F3}	0	p.u.
Rectifier loading factor, K_C	0.1	p.u.
Exciter demagnetizing factor, K_D	0.5	p.u.
Exciter time constant, T_E	0.3	s
Exciter constant related to self-exciter field, K_E	1	p.u.
Derivative maximum limit, VR_{max}	15.4	p.u.
Derivative minimum limit, VR_{min}	-15.4	p.u.
Maximum exciter output, VFE_{max}	6.3	p.u.
Minimum exciter voltage output, VFE_{min}	-6	p.u.

Power System Stabiliser

PSS2B Paramters used for the simulations are shown in the table B.3

Table B.3: PSS2B parameters

Parameter Description	Value
PSS2B gain, G_{pss}	20
Washout1 time constant, T_{w1}	5
Washout2 time constant2, T_{w2}	5
Washout3 time constant, T_{w3}	5
Washout4 time constant, T_{w4}	5
Lead1 time constant, T_1	0.17
Lag1 time constant, T_2	0.02
Lead2 time constant, T_3	0.17
Lag2 time constant, T_4	0.02
Lead3 time constant, T_{10}	0.17
Lag3 time constant, T_{11}	0.02
RTF parameter , M	5
RTF parameter, N	1
RTF time constant, T_9	0.1
RTF time constant, $T_8 = M.T_9$	0.5
Signal transducers time constant, T_{trans}	0.006
Integrator time constant, T_7	5

C

Appendix C

C.1 Notch Filter Investigation

The table C.1, C.2 and C.3 shows the stability margins for constant depth.

Table C.1: Constant Depth of -12dB

Notch	Depth (dB)	Width (Hz)	PM (Deg)	GM (dB)	Attenuation	RMS	Phase at 2Hz
1a	-12	0.5	90.1	17.2	10.898	0.2852	11.7
2a	-12	1	88.1	17.7	10.928	0.2842	11.5
3a	-12	1.18	84.5	17.9	10.932	0.2841	9.83
4a	-12	2	84.6	18.7	10.939	0.2838	8.03
5a	-12	3	81.6	19.7	10.966	0.282	5.74
6a	-12	6	73	22.3	12.35	0.241	0.93
7a	-12	10	69.8	25	13.06	0.222	-8.09
8a	-12	14.6	69.6	28	14.0	0.199	-14.8

Table C.2: Constant Depth of -17dB

Notch	Depth (dB)	Width (Hz)	PM (Hz)	GM (deg)	Attenuation	RMS	Phase at 2Hz
1b	-17	0.5	90.3	17.2	11.192	0.2057	11.5
2b	-17	1	88.1	17.9	11.176	0.2762	10
3b	-17	1.18	84	18	11.6769	0.2607	9.59
4b	-17	2	84	19	11.1315	0.2776	7.29
5b	-17	3	80.6	20.1	11.1127	0.2782	4.58
6b	-17	6	69.6	22.9	12.5376	0.2361	-3
7b	-17	8	66.9	24.5	12.884	0.2269	-7.87
8b	-17	10	65.1	26	13.2502	0.2175	-11.8
9b	-17	12.5	63.7	27.6	13.6883	0.2068	-16.5
10b	-17	15	63	29.1	14.0698	0.1979	-20.5

Table C.3: Constant Depth of -23dB

Notch	Depth (dB)	Width (Hz)	PM (Deg)	GM (dB)	Attenuation	RMS	Phase at 2Hz
1c	-23	0.5	90.4	13.1	11.2868	0.2727	11.3
2c	-23	1	88	13.5	11.2398	0.2742	9.79
3c	-23	1.18	83.5	13.5	11.223	0.2567	9.3
4c	-23	2	83.7	14.5	11.1558	0.2768	6.84
5c	-23	3	80	15.8	11.1007	0.2786	3.86
6c	-23	3.5	78.4	16.5			
7c	-23	3.7	77.8	17			
8c	-23	4	76.9	21.4			
9c	-23	6	67.5	23.3	12.579	0.235	-4.4
10c	-23	8	64.2	25	12.916	0.226	-9.55
11c	-23	10	62	26.6	13.3	0.2162	-14.1
12c	-23	12.5	60.1	28.3	13.778	0.2047	-19.4
13c	-23	15	59	29.9	14.193	0.195	-23.39

Now values for constant width are given below.

Table C.4: Constant Width of 6Hz

Notch	Depth (dB)	Width (Hz)	PM (Deg)	GM (dB)	Attenuation	RMS	Phase at 2Hz
1d	-4	6	83.5	19.7	7.3122	0.4309	6.15
2d	-6	6	80.9	20.6	8.3541	0.3822	3.79
3d	-8	6	78.9	21.3	8.882	0.3594	1.89
4d	-10	6	77.3	21.9	9.138	0.3492	0.13
5d	-12	6	73	22.3	12.35	0.241	-1.03
6d	-17	6	69.8	22.9	12.9	0.226	-3.01
7d	-20	6	68.6	22.3	12.98	0.551	-3.95
8d	-23	6	67.7	23.3	12.99	0.224	-4.6
9d	-25	6	67.2	16.1	12.98	0.224	-4.8
10d	-27	6	66.9	14.8	12.96	0.225	-4.89
11d	-30	6	66.5	13.8	12.94	0.303	-5.08
12d	-40	6	65.8	12.7	12.84	0.227	-5.65

Table C.5: Constant width of 9Hz

Notch	Depth (dB)	Width (Hz)	PM (Deg)	GM (dB)	Attenuation	RMS	Phase at 2Hz
1e	-4	9	83.2	20.8	7.4437	0.4244	3.67
2e	-6	9	80	22.1	8.5434	0.3740	0.13
3e	-8	9	77.3	23.1	9.1087	0.3504	-2.54
4e	-10	9	75	23.9	9.367	0.3401	-4.94
5e	-12	9	70.2	24.4	12.589	0.2347	-6.73
6e	-17	9	65.9	25.3	13.066	0.2220	-9.91
7e	-20	9	64.2	25.6	13.116	0.2209	-11.5
8e	-23	9	63	25.8	13.105	0.2212	-12
9e	-25	9	62.4	25.9	13.086	0.2217	-12.5
10e	-27	9	61.9	17.1	13.064	0.222	-12.9
11e	-30	9	61.4	15.4	13.032	0.2231	-13.1
12e	-35	9	60.8	14.2	12.989	0.2241	-13.5
13e	-40	9	60.4	13.8	12.963	0.2248	-13.6

Table C.6: Constant width of 12Hz

Notch	Depth (dB)	Width (Hz)	PM (Deg)	GM (dB)	Attenuation	RMS	Phase at 2Hz
1f	-4	12	83.8	21.6	8.432		1.83
2f	-6	12	80.1	23.3	10.123		-2.43
3f	-8	12	76.9	24.6	11.012		-6.05
4f	-10	12	74.2	25.5	11.478		-9.14
5f	-12	12	72	26.2	11.684		-11.5
6f	-17	12	63.9	27.3	13.605	0.2088	-15.7
7f	-20	12	61.9	27.7	13.684	0.2070	-17.2
8f	-23	12	60.5	28	13.687	0.2068	-18.4
9f	-25	12	59.7	28.1	13.672	0.2070	-18.9
10f	-27	12	59.1	20.2	13.653	0.208	-19.4
11f	-30	12	58.4	16.7	13.622	0.2084	-20.1
12f	-35	12	57.7	15.2	13.581	0.2094	-20.3
13f	-40	12	57.3	14.6	13.554	0.2100	-20.9